

PCCP

Accepted Manuscript



This is an *Accepted Manuscript*, which has been through the Royal Society of Chemistry peer review process and has been accepted for publication.

Accepted Manuscripts are published online shortly after acceptance, before technical editing, formatting and proof reading. Using this free service, authors can make their results available to the community, in citable form, before we publish the edited article. We will replace this *Accepted Manuscript* with the edited and formatted *Advance Article* as soon as it is available.

You can find more information about *Accepted Manuscripts* in the [Information for Authors](#).

Please note that technical editing may introduce minor changes to the text and/or graphics, which may alter content. The journal's standard [Terms & Conditions](#) and the [Ethical guidelines](#) still apply. In no event shall the Royal Society of Chemistry be held responsible for any errors or omissions in this *Accepted Manuscript* or any consequences arising from the use of any information it contains.



Physical Chemistry Chemical Physics

ARTICLE

Rebinding dynamics of NO to Microperoxidase-8 Probed by Time-resolved Vibrational Spectroscopy

Taegeon Lee,^{1a} Jooyoung Kim,^{1a} Jaeheung Park,^a Youngshang Pak,^a Hyojoon Kim^{*b} and Manho Lim^{*a}

Received 00th January 20xx,
Accepted 00th January 20xx

DOI: 10.1039/x0xx00000x

www.rsc.org/

Femtosecond vibrational spectroscopy was used to probe the rebinding kinetics of NO to microperoxidase-8 (Mp), an ideal model system for the active site of ligand-binding heme proteins, including myoglobin and hemoglobin, after the photodeligation of MpNO in glycerol/water (G/W) solutions at 294 K. The geminate rebinding (GR) of NO to Mp in viscous solutions was highly efficient and ultrafast and negligibly dependent on the solution viscosity, which was adjusted by changing the glycerol content from 65% to 90% by volume in G/W mixtures. The kinetics of the GR of NO to Mp in viscous solutions was well represented by an exponential function with a time constant of ca. 11 ps. Although the kinetic traces of the GR of NO to Mp in solutions with three different viscosities (18, 81, and 252 cP) almost overlap, they show a slight difference early in the decay process. The kinetic traces were also described by the diffusion-controlled reaction theory with a Coulomb potential. Since the ligand is deligated in a neutral form, an ionic pair of NO⁻ and Mp⁺ may be produced before forming the Mp–NO bond by an electron transfer from Mp to NO as the deligated NO is sufficiently near to the Fe atom of Mp. The strong reactivity between NO and ferrous heme may arise from the Coulomb interaction between the reacting pair, which is consistent with the harpooning mechanism for NO binding to heme.

Introduction

Reaction between heme and diatomic molecules such as NO, CO, and O₂ play an important role in the physiological functions of heme proteins such as myoglobin (Mb) and hemoglobin (Hb).¹⁻⁵ Knowledge of the reactivity of these molecules with heme is essential for fully understanding the functional mechanism of heme proteins involving small gas molecules. The rebinding of diatomic molecules to heme after the photodeligation of a ligated heme protein has been intensively studied to elucidate the reactivity and reaction mechanism of heme proteins with these molecules. The rebinding kinetics of CO to Mb at cryogenic temperatures was found to be highly nonexponential and complex, which was attributed to protein conformational relaxation and/or conformational inhomogeneity.⁶⁻¹¹ The rebinding of CO and NO to Mb and Hb after photodeligation of the ligated heme proteins in solutions with various viscosities at different temperatures has also been investigated to elucidate the protein conformational relaxation and its relation to ligand binding.¹¹⁻³¹

The rebinding of ligands to heme proteins can be complicated by ligand migration within the protein and protein conformational relaxation. Comparative studies on bare heme molecules such as iron protoporphyrin IX (FePPIX) have been performed to determine the intrinsic binding characteristics of the ligand to heme in the

absence of protein environments and conformational relaxation.³²⁻⁴⁰ The kinetics of CO rebinding to H₂O-FePPIX in viscous solutions has been found to be nonexponential, even though H₂O-FePPIX has no protein environment,³⁶⁻³⁹ suggesting that the nonexponential kinetics of CO rebinding is an inherent property of bare heme. The observed nonexponential kinetics in the solvated heme was attributed to either a distribution of the rebinding barriers^{39,41} or the diffusion of the deligated CO.³⁶ In contrast to the nonexponential and temperature-dependent rebinding of CO to H₂O-FePPIX, NO rebinding to H₂O-FePPIX was observed to be exponential and independent of temperature.³⁹ Although the nonexponential rebinding of CO to bare heme was well described by the diffusive motion of the deligated CO,³⁶ the diffusion model cannot explain the exponential rebinding of NO to bare heme; as a result, the diffusion model for ligand rebinding to heme was challenged.³⁹ Alternatively, a distribution of enthalpic barriers for the rebinding has also been suggested to be responsible for the nonexponential rebinding of CO.⁴¹ However, as the diffusive ligand failed to explain the exponential rebinding kinetics of NO, the distributed enthalpic barriers could not describe the rebinding kinetics of NO to bare heme using physically meaningful parameters.⁴² A harpoon mechanism that decouples NO rebinding from the heme conformation and the diffusion of the ligand near the heme resulting from the attractive interaction between the reacting pair was suggested to describe exponential NO rebinding.⁴³

In heme proteins, the active heme is covalently bonded to a proximal histidine in its fifth coordination site, and thus, a heme molecule coordinated to a proximal histidine is better suited for the active molecule of heme proteins than H₂O-FePPIX. In this regard, microperoxidase-8 (Mp), a heme octapeptide in which a proximal histidine is covalently bonded to the heme, is an excellent model system for the active molecule of heme proteins.⁴⁴ Mp constitutes a portion of a heme protein, cytochrome c, and was prepared by the

^a Department of Chemistry and Chemistry Institute of Functional Materials, Pusan National University, Busan, 46241 Korea

^b Department of Chemistry, Dong-A University, Busan, Korea

[†] Both authors contributed equally to this work.

^{*} To whom correspondence should be addressed.

Electronic Supplementary Information (ESI) available: [details of any supplementary information available should be included here]. See DOI: 10.1039/x0xx00000x

enzymatic digestion of cytochrome c. The rebinding of CO to Mp after the photodeligation of MpCO in solutions of various viscosities and different temperatures was measured to obtain the intrinsic reaction characteristics of CO binding to active heme in the absence of a specifically organized distal pocket and protein conformational substates.⁴² The GR of CO to Mp in viscous solutions was highly nonexponential. The GR rate and yield of CO to Mp increased with the viscosity of the solution. The viscosity-dependent kinetic behavior of CO rebinding to Mp was well reproduced by the pair survival probability function in the absence of any interaction potential between the geminate pair that was derived by the diffusion-controlled reaction model.³⁶ When the validity of the diffusion model in the absence of any interaction potential was further tested by applying the pair survival probability function to the rebinding of NO to Mp, it failed to reproduce the exponential kinetics observed in the NO rebinding.⁴² The harpoon model that successfully describes the rebinding kinetics of NO to the bare heme is based on an attractive interaction between the geminate pair. Thus, we have suggested that a diffusion model accommodating an attraction potential between the geminate pair can describe the kinetic behavior of NO rebinding.³⁶ Although the analytical form of the pair survival probability function in the presence of the interaction potential between the pair is not yet available, we were able to fit the kinetic data of NO rebinding to Mp using a pair survival probability function accommodating a Coulomb potential by numerical methods.

Here, we performed NO rebinding to Mp in solutions of three viscosities at room temperature to elucidate the reaction characteristics of NO with the active heme free from protein conformational substates and its relaxation after deligation. The GR of NO to Mp is exponential and almost independent of the viscosity of the solution used (18–252 cP). The rebinding kinetics of NO to Mp is well described by a diffusion-controlled reaction model incorporating a Coulomb potential between the geminate pair.

Materials and Methods

Femtosecond vibrational spectrometer

The details of the spectrometer are described elsewhere.⁴⁵ Briefly, a commercial Ti:sapphire regenerative amplifier (Hurricane, Spectra Physics) with a repetition rate of 1 kHz pumped by two identical home-built optical parametric amplifiers (OPA). One OPA generated a visible pump pulse at 575 nm with 3.5 μ J of energy by a frequency doubling of its signal pulse,⁴⁶ and the other OPA generated a tunable mid-IR probe pulse by difference frequency mixing of its signal and idler pulses.^{47,48} The isotropic absorption spectrum was obtained by setting the polarization of the pump pulse at the magic angle (54.7°) relative to the probe pulse. After passing through the sample, the broadband (~ 150 cm^{-1}) probe pulse was sent to a 320-mm monochromator with a 100-l/mm grating and then detected by a 64-element N₂(I)-cooled HgCdTe array detector mounted in the focal plane of the monochromator. The spectral resolution was ca. 1.6 cm^{-1} /pixel at 1660 cm^{-1} . A 12-bit analog-to-digital converter digitized the signals from each of the detector elements that were amplified with a home-built 64-channel amplifier. The pumped (A_p) and unpumped (A_u) absorbance values were obtained quasi-simultaneously by chopping the pump pulse at half the repetition frequency of the laser to calculate the pump-induced change in the absorbance of the sample ($\Delta A = A_p - A_u$). The pump-induced signal routinely exhibited less than 1.0×10^{-4} rms in absorbance units after 0.5 s of signal averaging when the IR light source was kept

stable (<0.3% rms). The probed region of the sample was uniformly photoexcited in space by keeping the pump spot sufficiently larger than the probe spot. The instrument response function was maintained at approximately 180 fs.

Sample preparation

Mp has a tendency to aggregate in solution, and the degree of aggregation is diminished by ligation, high pH, and the use of a solvent with low permittivity.^{40, 42, 44, 49-51} The MpNO sample was prepared in a glycerol/water (G/W) mixture at pH 12, and its concentration was kept low enough so that the MpNO would remain in the monomeric form.

Ferric Mp, Na₂S₂O₄, glycerol-d₃, and NO gas were purchased from Sigma-Aldrich Co. and used as received. A 2-mM ferric Mp stock solution was prepared in NaOD solution and diluted with an appropriate G/W mixture. The glycerol contents in the G/W mixtures were 65, 80, and 90% by volume, which corresponded to solution viscosities of 18, 81, and 252 cP, respectively, at 294 K.⁵² The diluted ferric Mp solution was deoxygenated by bubbling with N₂ gas, reduced by adding excess amounts of Na₂S₂O₄ powder, and ligated with NO by bubbling the gas until the solution turned red, which is the color of MpNO. Monomeric NO-ligated Mp (MpNO) was confirmed by UV-Vis and IR spectra of the sample.^{38,44} The final concentrations of MpNO and NaOD were 0.1 mM and 100 mM, respectively, resulting in a sample of pD = 12. The sample was passed through a gas-tight 110- μ m-path length flowing sample cell with two 2-mm-thick CaF₂ windows. The temperature of the cell was maintained at 294 ± 1 K by a circulating bath. D₂O and glycerol-d₃ were used to avoid overlap of the interested spectrum with the strong absorption bands related to the O–H moiety of the solvent.

Theory

The rebinding kinetics of CO to heme was explained by the theory of diffusion-influenced reaction in the absence of any interaction potential.^{36,42} However, the interaction potential effects should be taken into account when considering the kinetics of NO binding to heme.⁴² The general diffusion-reaction equation for a reacting pair under the interaction potential $U(r)$ is given by⁵³

$$\frac{\partial p(r,t)}{\partial t} = D \frac{1}{r^2} \frac{\partial}{\partial r} \left(r^2 e^{-\beta U(r)} \frac{\partial}{\partial r} (e^{\beta U(r)} p(r,t)) \right) \quad (1)$$

where $p(r,t)$ is the probability distribution function at the separation r at time t and $\beta = 1/k_B T$, where k_B is the Boltzmann constant, T is the absolute temperature, and D is the relative diffusion coefficient of the reacting pair. We consider the following initial condition,

$$p(r,0 | r_0) = \frac{\delta(r-r_0)}{4\pi r_0^2} \quad (2)$$

where $\delta(r)$ is the Dirac delta function and r_0 is the initial separation between the reacting pair. The radiation boundary condition describing the reaction at encounter is given by⁵⁴

$$k_D R e^{-\beta U(R)} \frac{\partial}{\partial r} (e^{\beta U(r)} p(r,t)) \Big|_{r=R} = k_0 p(R,t) \quad (3)$$

where R is the encounter radius, k_0 is the intrinsic rate constant of reaction at R , and $k_D = 4\pi R D$ for spherically symmetric diffusion. The left-hand side represents the radial flux on the boundary surface. Here, because NO reacts only from the distal side of the heme plane, as in the previous case of CO, a reactive hemisphere is assumed, such as $k_D = 2\pi R D$.^{36,42,55} Once the $p(r,t)$ is calculated, the pair survival probability function, $W(t)$, can be obtained by⁵³

$$W(t) = \int_R^\infty p(r, t) dr \quad (4)$$

We assumed that the interaction potential is the Coulomb potential, $U(r) = q_1 q_2 / 4\pi\epsilon r$, where q_1 and q_2 are the charges of the reacting particles and ϵ is the permittivity of the medium. The interaction potential was represented by the Onsager length $r_c = q_1 q_2 / 4\pi\epsilon k_B T$, resulting in $\beta U(r) = r_c / r$.⁵³ The survival probability function can be obtained by solving the diffusion-reaction equation, Eq. (1), with the conditions of Eqs. (2) and (3) in the Laplace transformed domain analytically⁵³ or numerically.^{56, 57} When numerically solving a parabolic-type partial differential equation, such as Eq. (1), for a very long time, employing the fourth-order Runge-Kutta method with adaptive time-step size control and the boundary-doubling method was found to be efficient.⁵⁷

Results

Figure 1 shows the vibrational absorption of NO in MpNO in viscous solutions at 294 K. The NO absorption band was well modeled by a Gaussian function centered near 1665 cm^{-1} with 32–40 cm^{-1} FWHM (full width at half maximum). It was blue-shifted from and broader than the NO band in MbNO or HbNO.⁴⁵ The broader vibrational band for the ligand in the ligated Mp was attributed to the exposure of the ligand to inhomogeneous solvent environments compared with the well-organized protein interior in heme proteins, where the NO band has much narrower vibrational band with 9–13 cm^{-1} FWHM.^{45, 58} The NO in the aggregated MpNO likely exhibits a different stretching mode compared with the monomer, resulting in several vibrational bands in the presence of aggregated MpNO. The single-featured vibrational bands obtained using the present sample conditions indicate that the prepared sample consists of monomeric MpNO.

Figure 2 shows representative time-resolved vibrational spectra of NO in MpNO after photodeligation of the MpNO in G/W mixtures at 294 K. The shape of the transient signal does not change, but its magnitude decays with time. The negative-going feature (bleach) arises from the loss of bound NO by photodeligation, and its magnitude represents the population of the deligated Mp at the given pump-probe delay. The magnitude of the initial bleach corresponds to ca. 1% MpNO photodeligation. Only a small fraction of the sample is photoexcited because of the sample's low concentration in the short path length sample cell. This low concentration was required to maintain MpNO in the monomeric form, and the short path length was chosen to minimize the background absorption of the solvent. Most of the bleach decays within 32 ps, suggesting that the GR of the deligated NO is rapid

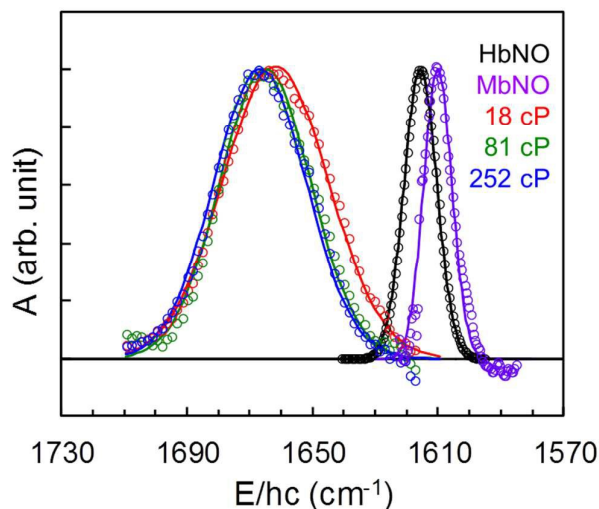


Figure 1. Equilibrium spectra of the NO stretching mode of MpNO in G/W mixtures at room temperature. The glycerol content in water was changed to vary the viscosity of the solution and was 65% (18 cP, red), 80% (81 cP, green), or 90% (252 cP, blue) by volume.⁵² Equilibrium spectra of HbNO (black) and MbNO (purple) in 70% G/W mixtures are also provided for comparison.⁵⁸ Data (open circles) were fit to a Gaussian function (solid lines).

and very efficient. The deligated Mp population was quantified by globally optimizing the entire set of spectra of a given sample using the Marquardt-Levenberg nonlinear least-squares fitting routine. An inverted Gaussian function was used to describe the bleach. Whereas the bandwidth and the center wavenumber of the Gaussian were globally optimized, the magnitude of the Gaussian was adjusted at each time point. The magnitude of the Gaussian represents the survival fraction of the deligated Mp after the photodeligation of MpNO. As shown in Figure 3, the kinetics of the magnitude decay was well described by an exponential function with a time constant of ca. 11 ps, and the time constant was nearly independent of the viscosity of the solution, indicating that the photodeligated NO geminately rebinds to Mp independently of the viscosity of the solution used.

The kinetics of NO rebinding to Mp was also fitted to the pair survival probability function derived from the diffusion-influenced bimolecular reaction in the presence of a Coulomb potential between the pair. The probability function, $W(t)$, was obtained by numerically solving Eqs. (1) and (4) using the fourth-order Runge-Kutta method with adaptive time-step size control and the boundary-doubling method.⁵⁷ The required parameters for solving

	CO			NO		
	19 cP	81 cP	252 cP	19 cP	81 cP	252 cP
R (Å)	1.36			1.36		
D (m^2/s)	5.67×10^{-11}	1.26×10^{-11}	4.04×10^{-12}	7.26×10^{-11}	1.61×10^{-11}	5.18×10^{-11}
k_0 (cm^3/s)	4.1×10^{-14}			4×10^{-14}		
r_0 (Å)	1.53	1.51	1.48	1.50	1.45	1.41
r_c (Å)	0			55	63	70

Table 1. Parameters of the pair survival probability functions for MpCO and MpNO. The parameters for MpCO are from reference 42 and those for MpNO were obtained in this work. The encounter radius (R) was assumed to be the same as that in MpCO and the diffusion coefficient was calculated from the D value of NO in water. Three parameters (k_0 , r_0 and r_c) were obtained by fitting MpNO data in three different viscosities. The Onsager length (r_c) is zero in MpCO as no interaction potential is present.

Eq. (1) are R , D , k_0 , r_0 , and r_c . We could not fit all these parameters independently because of the finite signal-to-noise ratio of the data and the limited number of data set, and thus, we utilized the parameters obtained in a previous experiment on MpCO. The GR kinetics of CO to Mp was well reproduced by the pair survival probability function without any interaction between the pair.⁴²

Because the size of NO is almost the same as that of CO, we assumed that R is the same in both MpNO and MpCO and used the reported value for MpCO.⁴² The value of R for MpCO was obtained by fitting several experimental data of MpCO in solutions of various viscosities at 294 K and at various other temperatures (283–323 K) to the analytical expression of the pair survival probability function derived from the diffusion-controlled reaction in the absence of any interaction potential. The R value was assumed to be an intrinsic property of the CO reaction with Mp and was found to be 1.36 Å. The R value in MpCO was fitted to be independent of the solvent viscosity and temperature. Here, we also assumed that R is an intrinsic property of the NO reaction with Mp, independent of the viscosity of the solution at 294 K, and the same as the R value of MpCO (1.36 Å). Although D represents the sum of the diffusion coefficients of Mp and NO, the diffusion of Mp is negligible, and thus, D is almost the same as the diffusion coefficient of NO, as is the case in MpCO.⁴² In MpCO experiment, D was reported to be $5.67 \times 10^{-11} \text{ m}^2/\text{s}$ at 18 cP solution and related to the viscosity (η) of the solution by $D \propto 1/\eta$.⁴² The D value of NO in water is known to

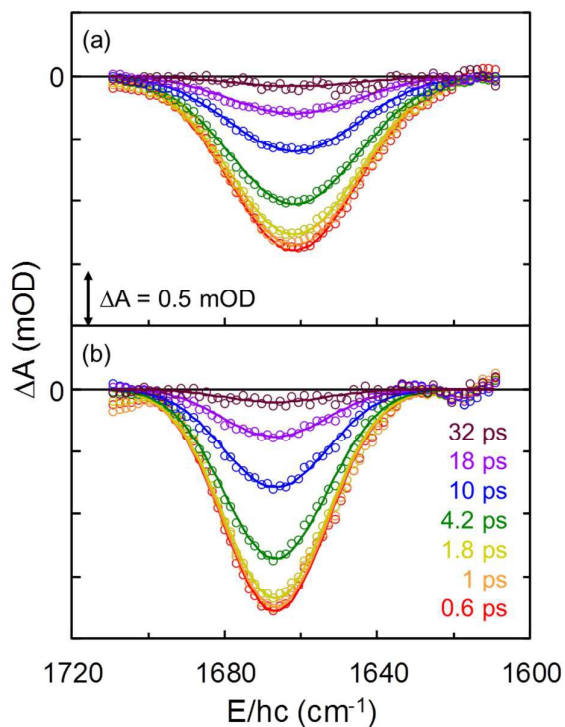


Figure 2. Representative time-resolved vibrational spectra of NO after the photodeligation of MpNO in 65% (a) and 90% (b) G/W (v/v) mixtures at 294 K. The featureless background arising from solvent absorption was modelled with a linear function and subtracted for better comparison. The remaining spectral feature (open circles) was well described by a Gaussian function (solid lines). The negative absorption arises from the loss of bound NO after photodeligation, and the magnitude of the signal is proportional to the population of the photodeligated MpNO at the given time delay. The ordinate, ΔA , is the absorption difference between the samples after and before photodeligation. The optical density (OD) unit is given in mOD (1 mOD = 10^3 OD) for small absorption differences. The pump-probe delays are 0.6, 1, 1.8, 4.2, 10, 18, and 32 ps (bottom to top) and are colour coded.

be 28% larger than that of CO in water. Thus, we set the D value for MpNO to be 1.28 times that for MpCO and inversely proportional to the viscosity of the solution: $D = 7.26 \times 10^{-11} \text{ m}^2/\text{s}$ at 18 cP, $1.61 \times 10^{-11} \text{ m}^2/\text{s}$ at 81 cP, and $5.18 \times 10^{-12} \text{ m}^2/\text{s}$ at 252 cP solution. Using the fixed R and D s values, we fit data from three viscous solutions (18, 81, 252 cP) to optimize k_0 , r_0 , and r_c . In MpCO, k_0 was an intrinsic property of the reaction and independent of the viscosity of the solution. The r_0 in MpCO decreased from 1.53 to 1.51 and then to 1.45 Å as the viscosity of the solution increased from 18 to 81 and then to 252 cP. Here, we also assumed that k_0 is an intrinsic property of the NO reaction with Mp and independent of the viscosity of the solution and that r_0 is related to the solution viscosity. We optimized r_0 for the kinetic trace in a solution of 18 cP and fixed r_0 for the kinetic traces in solutions with other viscosities by scaling it to the reported r_0 of MpCO in the solution with the same viscosity. The Onsager length r_c is dependent on the permittivity of the solution, which varies with the composition of the G/W mixture. Because the permittivity of D₂O was almost the same as that of H₂O,⁵⁹ the permittivity of the G/W mixtures using deuterated solvents was considered to be approximately that of a G/W mixture without isotope substitutions, which was estimated from the experimentally available values for various G/W compositions. The estimated relative static permittivities (ϵ_{0r}) are 58, 50, and 45 for solutions with $\eta = 18, 81,$ and 252 cP, respectively, at room temperature.⁶⁰ For monovalent ions at 294 K, the Onsager length is calculated to be 9.8 Å in 18 cP, 11.3 Å in 81 cP, and 12.5 Å in 252 cP. As the glycerol content in the G/W mixture increases, the viscosity of the solution increases, the ϵ_{0r} decreases, and the Onsager length increases, implying that the attractive interaction becomes stronger.

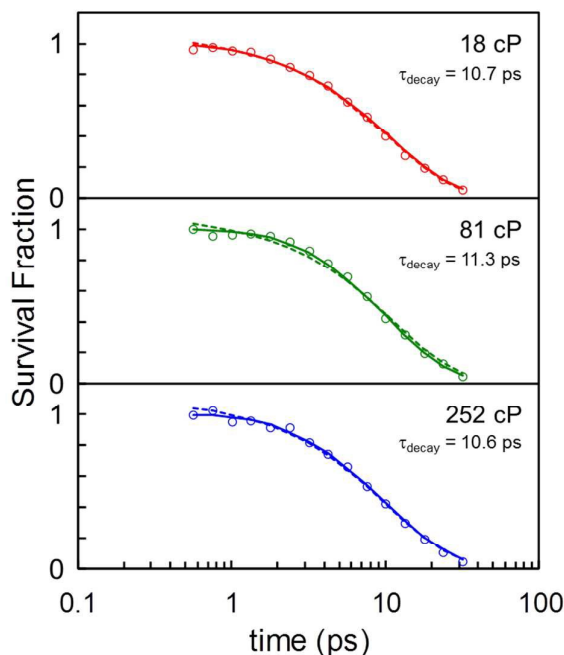


Figure 3. Kinetics of survival fraction of deligated heme after photodeligation of MpNO in the 18 cP (red), 81 cP (green), and 252 cP (blue) solutions at 294 K. The kinetic data (open circles) were fit to an exponential function with time constants of about 11 ps (dashed lines) as well as the theory of diffusion-controlled reaction in the presence of a Coulomb attractive potential (solid lines).

As mentioned previously, 5 parameters (R , D , k_0 , r_0 , and r_c) were required to calculate $W(t)$, and these 5 parameters were globally applied to fit all of the decay kinetics in solutions with various viscosities. The values for R and k_0 are the same for all the kinetic traces. Although the values for D , r_0 , and r_c were global, D and r_0 varied with the viscosity and r_c varied with the permittivity of the solution. First, we related the R and D values to the previous fitting of MpCO and fixed them. Then, we optimized the remaining three parameters to fit all the kinetic traces of MpNO. The best fitting values were $k_0 = 4 \times 10^{-14} \text{ cm}^3/\text{s}$, $r_0 = 1.5 \text{ \AA}$, and $r_c = 55 \text{ \AA}$ for the 18-cP solution (see Table 1). Except k_0 , r_0 and r_c varied with the viscosity of the solution and exhibited values of 1.41 and 70 \AA , respectively, in the 252-cP solution. A much larger r_c was needed to fit the data than the value calculated using ϵ_{0r} . However, since the permittivity depends on the frequency of the applied electric field, and the permittivities of water and glycerol at high frequencies can be 1/45 and 1/12 of the static value, respectively,^{61, 62} the fitted Onsager length, which required the relative permittivity (ϵ_r) to be $\epsilon_r = \epsilon_{0r} / 5.6$, is certainly feasible (see the Discussion section).

Considering that only three global parameters (k_0 , r_0 and r_c) were adjusted to fit all three kinetics traces, the consistency between the experimental GR kinetic data and the theoretical predictions is remarkable (see Figure 3). For a higher viscosity solution, the diffusive encounter occurs more slowly, but the shorter initial separation and the stronger attraction field cause the reactions to occur more rapidly. Because these effects are contradictory, the survival probability curves do not show much difference, unlike those in the case of CO without an interaction potential. Note that the attraction field effect dominates the long-term kinetics, namely, $S(\infty) \approx \exp(-r_c/r_0)$, as predicted by Onsager,⁶³ while this relation was $S(\infty) = 1 - \frac{R}{r_0} \frac{k_0}{k_D + k_0}$ for CO. $S(\infty)$ represents the fraction of the escaped ligand without GR after photodeligation of the ligated molecule. Because $r_c/r_0 \ll 1$ for the reaction of NO with Mp, the escaped fraction of NO without GR after the photodeligation of MpNO is negligible, as was observed. For MpCO, where there is no interaction potential between Mp and CO, a large fraction of the photodeligated CO escapes without GR. Therefore, Figure 3 clearly demonstrates the existence of a strong attraction field between Mp and NO.

Discussion

Because the heme was excited by a 575-nm photon, the energy of which (208 kJ/mol) is much larger than the bond energy of the Fe–NO of heme (113–125 kJ/mol),^{64, 65} the excess energy should be distributed into Mp and the deligated NO upon photolysis of MpNO. The energy in the NO will be distributed amongst its vibrational, rotational, and translational motions, and thus, when more energy is deposited into the vibrational or rotational motion of the deligated NO, it will have less translational energy. The NO with excess translational energy will fly off the Mp upon the photodeligation of MpNO. A molecular dynamics (MD) simulation has shown that the photodeligated NO from MbMO with excess kinetic energy is thermalized within 0.3 ps and that its motion subsequently becomes diffusive.⁶⁵ Therefore, the detached NO likely exhibits diffusive thermal motion shortly after

photodeligation, even if it has flown off of Mp because of excess kinetic energy. In the MpCO experiment, diffusive motion well described the behavior of the photodeligated ligand that flew off because of excess kinetic energy. The photodeligated ligand that flew off achieved greater initial separations in less viscous solutions. If there is no attractive interaction between NO and Mp, the diffusive NO will drift away from the Mp, and in less viscous solutions, the diffusion will be more rapid, resulting in slower, less frequent GR, as observed in the GR kinetics of MpCO. However, although the initial separation and diffusion rate depend on the viscosity of the solution, the GR kinetics of NO to Mp in various viscous solutions converges as time passes (see Figure 4), indicating that GR is dictated not by the diffusive motion but instead by the attractive interaction. We calculated the GR kinetics of NO to Mp when there is no attractive interaction between NO and Mp by setting $r_c = 0$ and keeping all other parameters the same. As can be seen in Figure 4, the calculated GR kinetics with $r_c = 0$ (the dotted lines) heavily depends on the viscosity of the solution, more NO rebinds faster in more viscous solution, which is consistent with the observed GR kinetics of CO to Mp⁴² but inconsistent with the experimental GR kinetics of NO to Mp.

The fitted Onsager lengths of 55–70 \AA are 5.6 times larger than the calculated values of 9.8–12.5 \AA using static permittivity. As mentioned previously, the permittivity depends on the frequency of the applied electric field. Since the photodeligated ligand from MpNO is a neutral NO (*vide infra*), the reacting pair (Mp, NO) experiences the Coulombic interaction only after a charged pair is formed. A charged pair can be formed by an electron transfer from Mp to NO. The permittivity can be conceived of as the ability to diminish the Coulomb interaction between charged compounds by rearranging the charge distribution of the surrounding solvent molecules. When the charged pair is formed after an electron transfer, the static permittivity is not appropriate for calculating the immediate Coulomb interaction between the newly formed charged pair. Because the GR time constant of NO to Mp is approximately 11 ps, the electron transfer should occur earlier than

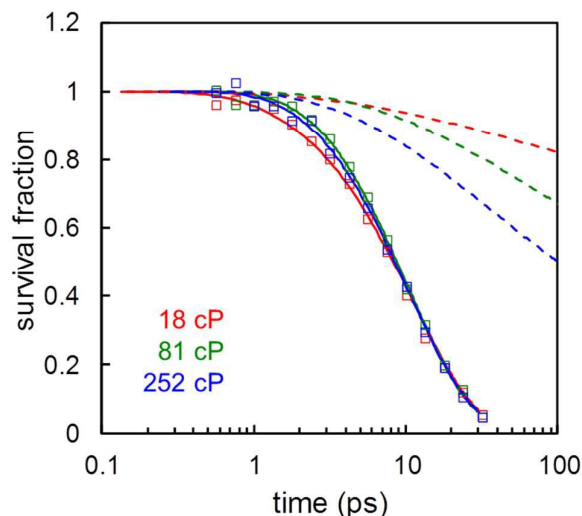


Figure 4. Simulated kinetics of the survival fraction of deligated heme after the photodeligation of MpNO in 18-cP (red), 81-cP (green), and 252-cP (blue) solutions when the Coulomb attraction was removed by setting $r_c = 0$ (dashed lines) while keeping all other parameters equal to the best fit. When the Coulomb interaction is absent, the GR of the deligated NO to Mp becomes slower, and its kinetics depends on the viscosity of the solution, as observed for the GR of CO to Mp. For comparison, GR kinetic data (open squares) of NO to Mp are also shown with their best fits (solid lines).

11 ps, as if the electric field is produced at a frequency exceeding 91 GHz. Using the reported frequency-dependent permittivities of G/W mixtures at 265.5 K,⁶⁶ the ϵ_r values of 82% and 90% G/W (v/v) mixtures at 265.5 K are calculated to be 4.3 and 4.1 at 100 GHz, respectively; furthermore, both of these values approach the asymptotic value of 4 at 1000 GHz. Based on the temperature-dependent permittivity of glycerol,⁶² the ϵ_r values of glycerol at 265 K and 285 K are calculated to be 4.7 and 5.3 at 2 GHz; both reach 4.1 at 100 GHz and approach 4 at 1000 GHz. The permittivity of G/W mixtures quickly approaches the value of pure glycerol as the frequency or the glycerol content increases.⁶⁶ Although the frequency-dependent ϵ_r values of G/W mixtures at 294 K are not available, we were able to estimate them by extrapolating the parameters to calculate the frequency-dependent permittivity from the reported experimental measurements.^{62, 66} The estimated ϵ_r value for the Mp + NO reaction in G/W mixtures could be as small as 4.6–4.1, lower than the static value of 58–45. Clearly, the Onsager length can be as large as 11 times the calculated r_c using the static permittivity. Thus, the fitted r_c value, which requires ϵ_r to be 10.4–8, is certainly within the range of the feasible permittivity of the G/W mixture. The GR kinetic data of NO to Mp were also reproduced when fitted by fixing r_c to the calculated value using $\epsilon_r = 4.6$ –4.1 by adjusting only k_0 to be $1.8 \times 10^{-14} \text{ cm}^3/\text{s}$.

Although an attractive interaction between NO and Mp is crucial to explain the observed GR kinetics of NO to Mp, the MpNO does not appear to photodissociate into ionic species, i.e., NO^- and Mp^+ . When MbNO or HbNO was photoexcited with a 575-nm photon, the neutral ligand NO, not NO^- , has been directly observed.^{58, 67, 68} When $\text{H}_2\text{O-FePPiX-NO}$ or MbNO was photoexcited by a 580-nm photon, ferrous heme, not ferric heme, has been shown to appear immediately upon photodeligation.⁶⁹ Therefore, MpNO should photodissociate into the neutral species NO and Mp. A neutral pair can attract each other when an electron from one molecule is transferred to the reacting partner, thus generating an ionic pair before the bond is formed. The textbook description of the harpoon mechanism underlying the gas-phase reaction indicates that an electron can be transferred from a molecule (donor) to the reacting partner (acceptor) if the distance between the reacting pair is within the harpoon distance (r_H) defined by $IE - EA - e_2/4\pi\epsilon_0 r_H < 0$, where ϵ_0 is the permittivity of the vacuum and e is the electronic charge.⁷⁰ Here, IE and EA represent the ionization energy of the donor and the electron affinity of the acceptor compound, respectively. In the solution phase, we may define the r_H that satisfies the equation $\Delta G_{\text{acceptor}}^{\circ} + \Delta G_{\text{donor}}^{\circ} - e_2/4\pi\epsilon_r r_H < 0$, where $\Delta G_{\text{acceptor}}^{\circ}$ and $\Delta G_{\text{donor}}^{\circ}$ are the standard reaction Gibbs energies of the half reactions to accept and donate an electron, respectively.

In the case of MpNO in G/W mixtures, $\Delta G_{\text{acceptor}}^{\circ}$ and $\Delta G_{\text{donor}}^{\circ}$ are the standard reaction Gibbs energies of $\text{NO} + e^- \rightarrow \text{NO}^-$ and $\text{Mp} \rightarrow \text{Mp}^+ + e^-$ in solution, respectively, when each compound is at a concentration of 1 M. These values are simply related to the standard reduction potentials of NO and Mp^+ as follows,

$$\Delta G_{\text{acceptor}}^{\circ} = -FE^{\circ}(\text{NO}/\text{NO}^-)$$

$$\Delta G_{\text{donor}}^{\circ} = FE^{\circ}(\text{Mp}^+/\text{Mp}),$$

where F is the Faraday constant and $E^{\circ}(\text{NO}/\text{NO}^-)$ and $E^{\circ}(\text{Mp}^+/\text{Mp})$ are the standard reduction potentials of NO and Mp^+ , respectively, when all the compounds are at concentrations of

1 M. Therefore, the reduction potential was given for 1 M of compounds versus normal hydrogen electrode hereafter. EA of NO has a slightly positive value of 0.026 eV,⁷¹ but $E^{\circ}(\text{NO}/\text{NO}^-)$ has a negative value of -0.8 V ,⁷² suggesting that the reduction of NO is spontaneous in the gas phase but nonspontaneous in solution. $E^{\circ}(\text{Mp}^+/\text{Mp})$ was reported to be 0.34 V at pH = 7.4,⁷³ but it is not known at pH = 12, which was the pH used here. Similar to Mp^+ , the reduction potential of ferric cytochrome c was found to decrease as the pH of the solution increased and is near zero when the solution pH = 12.⁷⁴ Thus, $E^{\circ}(\text{Mp}^+/\text{Mp})$ should be smaller than 0.34 V and could be near zero at pH = 12. For the reaction of $\text{Mp} + \text{NO} \rightarrow \text{Mp}^+ + \text{NO}^-$ in solution, $\Delta G_{\text{acceptor}}^{\circ} + \Delta G_{\text{donor}}^{\circ}$ were calculated to be 77–110 kJ/mol using the reported reduction potentials of $E^{\circ}(\text{NO}/\text{NO}^-) = -0.8 \text{ V}$ and $0 \text{ V} \leq E^{\circ}(\text{Mp}^+/\text{Mp}) < 0.34 \text{ V}$, resulting in $r_H = 3.1$ –4.4 Å in $\epsilon_r = 4.1$ solution and $r_H = 1.3$ –1.8 Å in $\epsilon_r = 10$ solution. As long as the solution has $\epsilon_r < 8.4$, the harpoon mechanism can function in the Mp–NO bond formation because r_H exceeds 1.5 Å (the largest initial separation in MpNO) when $\epsilon_r < 8.4$. As discussed previously, $\epsilon_r < 8.4$ is within the feasible ϵ_r range of the G/W mixtures used here when the dynamics nature of the induced electric field is taken into account. Although the reduction of NO is unfavorable in solution, the GR kinetics of NO to Mp indicates that an electron of Mp can be transferred to NO within the harpoon distance, producing the ionic reacting pair, Mp^+ and NO^- , before forming the Mp–NO bond. Because NO^- is readily formed in the gas phase (as can be seen from the positive value of EA for NO), the electron transfer from Mp to the geminate NO appears to be both kinetically and thermodynamically feasible.

The GR process following the photodeligation is highly nonequilibrium process but we calculated the energetics of the electron transfer from Mp to NO using the equilibrium Gibbs energy. Furthermore, the positive charge in Mp might be delocalized over the heme. Thus the calculated energetics is a rough estimate for the electron transfer. However, it may be the only way to check the energetic feasibility of the electron transfer without running atomistic MD simulation. Atomistic MD simulations may show the nonequilibrium energetics as well as the detailed charge distribution in the heme needed to estimate the realistic energetics for the electron transfer.

NO is deligated in a neutral form and the fast rebinding of NO to Mp was well described by the diffusion-controlled reaction theory in the presence of a Coulomb potential. The electron transfer from Mp to NO appears to be feasible energetically as long as the reacting pair are within the harpoon distance, which can be as large as 4 Å. Thus the deligated NO diffuses around in a neutral form before an electron is transferred from Mp to NO, producing ionic pair (Mp^+ and NO^-). Once the ionic pair is formed, the Coulombic attraction between two ions starts to dominate and induces a rapid formation of the Fe–NO bond. Clearly, if happens, the electron transfer precedes the formation of the bond. We have shown that the electron transfer is feasible thermodynamically but the time constant for the electron transfer, which should be smaller than 11 ps, is not recovered in the present model.

In the diffusion-controlled reaction theory with a Coulomb potential, the reacting pair is charged all the time during diffusion. However, the deligated ligand from MpNO is the neutral NO and is charged by an electron transfer when it is within the harpoon distance from Mp. Therefore, more realistic model for the GR of NO to Mp may be the diffusion-controlled reaction theory with a Coulomb potential that is turned on with a certain time constant.

Before such a model is available, the fitted parameters obtained here can be used as a rough estimate for the corresponding parameters.

When the NO^- and Mn^+ are formed during the rebinding, can their spectroscopic features be observed? With the time-resolved IR spectroscopy, we see the spectroscopic feature when a measurable fraction of a compound is accumulated at some point in time.⁷⁵ When population of an intermediate is sufficient to be observed at a given time, its spectroscopic marker will show up.⁷⁶ Vibrational spectrum of NO^- can be observed only when the NO^- either forms simultaneously in a sufficient quantity or is accumulated enough at a given time. As discussed, the NO diffuses around in a neutral form and becomes NO^- via electron transfer before forming the Mn–NO bond. Since the NO^- forms asynchronously and the produced NO^- disappears quickly due to the MnNO formation, NO^- cannot be accumulated in a sufficient quantity to be observable and thus, its vibrational spectrum is unlikely detectable. Even the population of NO^- is accumulated enough at some point in time, its vibrational band is observable only when its absorptivity of NO^- is large enough to be detected. The absorptivity of the vibrational band of NO^- is not known but that of NO is about 30 times smaller than that of NO-bound to heme.⁵⁸ The vibrational band of the deligated NO in solution has not been detected yet due to low absorptivity and possibly broad band width. If the absorptivity of the vibrational band of NO^- is similar to that of the deligated NO, even all the deligated ligand becomes NO^- , the magnitude of the vibrational spectrum of NO^- is too small to be detected in our experimental conditions.

As mentioned previously, the photodeligated NO will fly off from Mn, and its motion will become diffusive rapidly because of collisions with the surrounding solvent molecules. We defined the initial separation to be the distance at which the photodeligated NO loses its excess translational energy and begins to exhibit diffusive motion. As the kinetic energy of the detached NO increases, the initial separation from Mn increases, and r_0 thus also increases. Because there will be a distribution of initial separation, the value of r_0 represents an average of the initial separations achieved by NO after photodeligation. The initial separation of the photodeligated NO from MnNO ranges from 1.5 to 1.41 Å, which is slightly smaller than that of the photodeligated CO from MnCO (1.53–1.45 Å). This range is consistent with the reported population of the vibrationally excited ligand after the photolysis of ligated Mb, a similar heme system. When MbNO and MbCO were photoexcited by a 575-nm photon, approximately 15% of NO^{67} and 6% of $\text{CO}^{77,78}$ respectively, were deligated in the vibrationally excited state. When the same energy is deposited into the deligated ligand, as more energy is partitioned into its vibrational energy, less energy will be partitioned into its translational energy, resulting in a smaller initial separation. Because more NO than CO is vibrationally excited when detached from heme, a greater proportion of NO will likely exhibit less excess kinetic energy as long as the similar amount of energy is deposited into the deligated ligand and thus achieve shorter average separations after thermalization.

The value for the encounter radius, $R = 1.36$ Å, which we assumed to be the same as in MnCO, is even shorter than the Fe–N bond length of 1.74 Å.⁶⁵ The encounter radius should be at least the distance between the Fe and the center of the NO molecule. The NO molecule should both have the appropriate orientation to form the Fe–NO bond and be within reacting distance. The fitted encounter radius was underestimated because some NO molecules within the bonding distance cannot bind to Mn because of

improper orientation. Thus, the value for the encounter radius, 1.36 Å represents a value at least 1.74 Å in reality. In the same logic, the fitted initial separation should be larger than 1.74 Å. Using a simple scaling, r_0 of 1.5 ~ 1.41 Å represents the value of at least 1.92 ~ 1.8 Å, suggesting that the initial separation of the deligated NO is about 2 Å from the Fe. The intrinsic rate constant at the encounter distance of NO and Mn is almost equivalent to or smaller than that of CO and Mn, suggesting that the more rapid GR of NO to Mn is not attributable to the more rapid intrinsic rate constant but is instead due to the attractive interaction resulting from the electron transfer that occurs before bond formation.

As mentioned previously, the deligated NO can be charged by an electron transfer from Mn when the initial separation between Mn and NO is shorter than the harpoon distance. However, if the initial separation is large enough to prohibit the electron transfer, the NO will diffuse away, and GR will become less efficient. A large initial separation is expected in low viscosity solutions. Our preliminary data on NO rebinding to Mn in methanol ($\eta = 0.544$ cP) showed that approximately 70% of the deligated NO geminately rebound with a time constant of ca. 7 ps and that the remainder escaped without GR. This observation indicates that a portion of the deligated ligand achieved a sufficient initial separation to prevent the occurrence of electron transfer in low viscosity solution. The neutral ligand exhibits purely diffusive motion and drifts away from Mn. As observed in the MnCO experiment, the deligated ligand did not geminately rebound to any extent in low viscosity solution because of its rapid diffusion away from Mn.⁴²

Whereas the deligated NO can geminately rebound to Mn in an ionic form under the influence of Coulomb attraction because of the transfer of an electron from Mn to NO before the formation of the Mn–NO bond, the deligated CO geminately rebounds to Mn through pure diffusion of the neutral CO. Why can NO generate an ionic pair with Mn before forming the bond but CO cannot? The reduction potential of NO was calculated from its EA and the solvation energies of NO^- and NO using the known reduction potential of O_2 as a reference value.⁷² The reduction potential of CO, $E^\circ(\text{CO}/\text{CO}^-)$, which is not known, was estimated from its EA (-1.326 eV)⁷⁹ and the solvation energies of CO^- and CO using $E^\circ(\text{NO}/\text{NO}^-)$ as a reference value. The solvation energies of CO^- and CO, which were calculated using the polarizable continuum model⁸⁰ by B3LYP with the 6-311+G* basis set^{81,82} in G/W mixtures, were 25–33 kJ/mol higher than those of NO^- and NO. Thus, $E^\circ(\text{CO}/\text{CO}^-)$ was estimated to be a larger negative value than -2.4 V. Using the estimated $E^\circ(\text{CO}/\text{CO}^-)$, $\Delta G_{\text{acceptor}}^\circ + \Delta G_{\text{donor}}^\circ$ for the reaction of $\text{Mn} + \text{CO} \rightarrow \text{Mn}^+ + \text{CO}^-$ in solution was calculated to be larger than 231 kJ/mol, and therefore, $r_H < 1.46$ Å in $\epsilon_r = 4.1$ solution and $r_H < 0.6$ Å in $\epsilon_r = 10$ solution. Because the initial separation between Mn and CO exceeds 1.45 Å, the electron transfer from Mn to CO is thermodynamically unfavorable. Furthermore, highly unstable gas-phase CO^- may also kinetically hinder the formation of CO^- . In contrast to NO^- , the formation of CO^- appears to be both kinetically and thermodynamically unfavorable, which is likely the underlying reason for the purely diffusional rebinding of CO to Mn.

The reduction potential of O_2 is -0.16 V,⁷² implying that, although unfavorable, O_2^- can be much more readily formed in solution than NO^- . Because the EA of O_2 exhibits a positive value of 0.451 eV,⁸³ O_2^- is highly favorable in the gas phase. Thus, an electron transfer from Mn to O_2 in solution is certainly kinetically

and thermodynamically feasible. As long as the separation between the neutral Mp and O₂ is sufficiently small, an electron can be transferred from Mp to O₂, resulting in an ionic pair of Mp⁺ and O₂⁻. Once the ionic pair is produced, the GR kinetics of O₂ to Mp would be as rapid and efficient as that of NO to Mp. However, if the initial separation is large because of the low viscosity of the solution and the electron transfer is thus kinetically prohibited, the deligated O₂ will diffuse away without GR. According to the GR kinetics of O₂ to picket fence heme in toluene ($\eta = 0.59$), only a fraction of the deligated O₂ geminately rebinds, and the GR kinetics occurs on the picosecond time scale.⁸⁴ Clearly, the GR of O₂ to heme can be described by the reaction between the charged pair generated by an electron transfer from the heme to O₂ when they are sufficiently close. In fact, because O₂⁻ readily forms in solution because of the low reduction potential of O₂, O₂-ligated heme is relatively unstable.⁸⁵ For example, Mp⁺ + O₂⁻ in solution can be more stable than MpO₂ if Mp⁺ is stabilized by an interaction, such as the coordination of water to Mp⁺. Indeed, when MpO₂ sample preparation was attempted by adding O₂ to Mp, oxidized heme (Mp⁺) was formed instead of MpO₂. O₂-ligated hemes, such as oxy heme proteins and picket fence heme, can be formed when they are stabilized by blocking the attack of nucleophilic species or forming a hydrogen bond with a side chain.^{84,85}

To test the validity of the $W(t)$, the pair survival probability function derived from the diffusion-influenced bimolecular reaction with a Coulomb interaction used to describe the GR kinetics of NO to heme, we simulated the GR kinetics of NO to H₂O-FePPiX in the temperature range of 290–200 K and observed exponential and almost temperature-independent kinetics (Figure 1B in Ye et al.³⁹). During the simulation, R and k_0 were set to be the same as the best fitted parameters for MpNO in solutions of various viscosities at 294 K. Additionally, r_0 and D were scaled to the viscosity of the solution, and r_c was adjusted for the permittivity of the solution and temperature. As can be seen in Figure 5, the simulated data reasonably reproduce the experimental observation that GR kinetics is exponential and almost independent of temperature, which supports the validity of the model and fitted parameters. Because k_0 was found to depend on temperature in the GR of CO to H₂O-FePPiX, a better simulation can be obtained by adjusting k_0 .

Although the harpoon mechanism well describes the kinetics of NO rebinding to Mp, it might be a specific property of Mp reacting with NO. More works are required to generalize the harpoon mechanism to the reaction of NO with Mb and Hb.

Fast and exponential rebinding of NO to a model heme was suggested to arise from the bonding of NO to the domed heme.⁶⁹ Binding of NO to the domed heme was observed in various heme proteins.⁸⁶ The binding of NO to the domed heme was attributed to the electronic property of NO such that it has an unpaired electron, which enables NO to form a bond with the electron in the d_{z^2} orbital of high-spin Fe(II) atom in the domed heme.⁶⁹ It was consistent with a density functional theory calculation showing that the intermediate spin state of NO is a bound state.⁸⁷ Although the kinetics of NO rebinding to Mp is well described by the diffusion-controlled reaction with a Coulomb potential and the electron transfer from Mp to NO is thermodynamically feasible, there is no direct evidence for the formation of the ionic pair (Mp⁺, NO⁻). Thus, the Coulomb attraction in the diffusion model may be not due to the formation of the ionic pair but simply reflect the electronic property of NO leading to its fast binding to the domed heme.

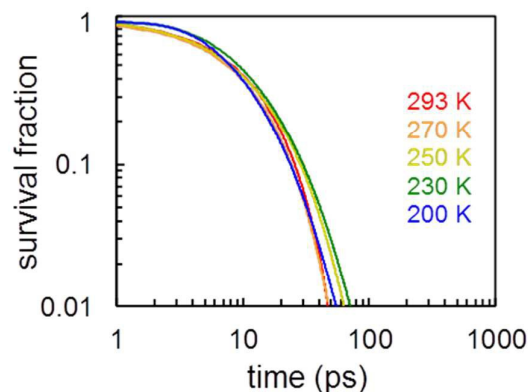


Figure 3 Simulated kinetics of NO rebinding to H₂O-FePPiX at 290 (red), 270 (orange), 250 (pink), 230 (green), and 200 K (brown). The pair survival probability function, $W(t)$, was calculated by properly adjusting the best fitted parameters for MpNO at 294 K; R and k_0 were kept the same, r_0 and D were scaled to the viscosity of the solution, and r_c was adjusted for the permittivity of the solution and temperature.

Conclusions

NO rebinding kinetics with Mp after the photodeligation of MpNO in three viscous solutions was investigated at 294 K using femtosecond infrared spectroscopy. The GR of photodeligated NO to Mp is ultrafast, highly efficient, and almost independent of the viscosity of the solution. Most of the photodeligated NO geminately rebinds to Mp with a time constant of ca. 11 ps, and the geminate yield is near unity. The GR kinetics was well described by the diffusion-influenced bimolecular reaction in the presence of a Coulomb potential between the reacting pair. When MpNO is photoexcited, the ligand is detached in a neutral form, but an electron can be transferred from Mp to NO when they are within the harpoon distance, producing the ionic pair, Mp⁺ and NO⁻, before the Mp-NO bond forms. The Coulomb attraction between the ionic pair may be responsible for the rapid and efficient GR of NO to Mp. The viscosity-independent GR kinetics of NO to Mp indicates that the Coulomb attraction dominates the diffusional motion of the deligated NO.

Acknowledgements

This work was supported by the National Research Foundation of Korea (NRF) grant funded by the Korea government (MEST) (NRF-2014R1A2A2A01002456, NRF-2014R1A4A1001690). J. Kim was supported by the 2014 Post-Doc Development Program of Pusan National University.

References

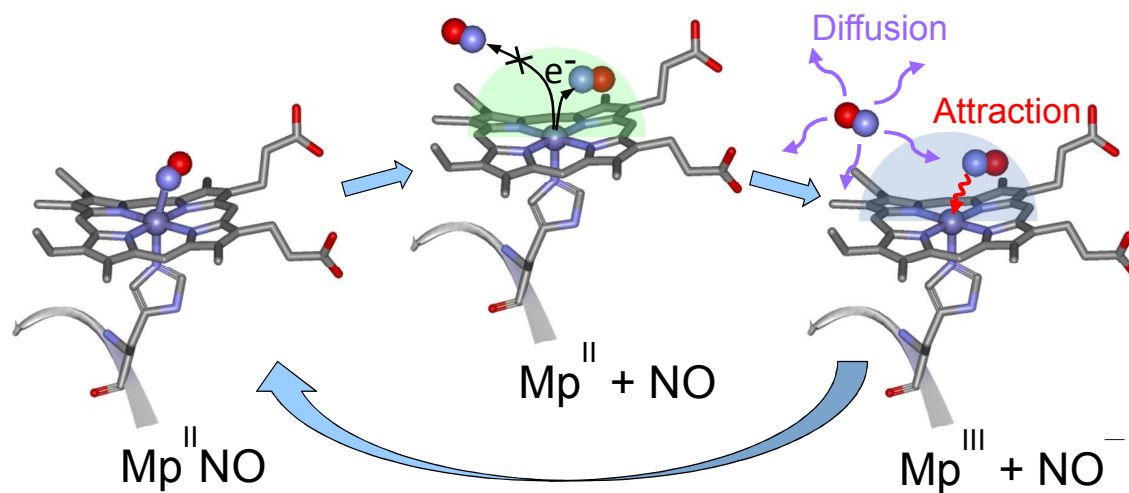
- 1 E. Antonini and M. Brunori, *Hemoglobin and Myoglobin in Their Reactions With Ligands*, North-Holland Publishing Company, London, UK, 1971.
- 2 L. Jia, C. Bonaventura, J. Bonaventura and J. S. Stamler, *Nature*, 1996, **380**, 221-226.

- 3 S. Moncada and A. Higgs, *N. Engl. J. Med.*, 1993, **329**, 2002-2012.
- 4 C. Nathan, *FASEB Journal*, 1992, **6**, 3051-3064.
- 5 J. S. Stamler, D. J. Singel and J. Loscalzo, *Science*, 1992, **258**, 1898-1902.
- 6 R. H. Austin, K. W. Beeson, L. Eisenstein, H. Frauenfelder and I. C. Gunsalus, *Biochemistry*, 1975, **14**, 5355-5373.
- 7 A. Ansari, J. Berendzen, D. K. Braunstein, B. R. Cowen, H. Frauenfelder, M. K. Hong, I. E. T. Iben, J. B. Johnson, P. Ormos, T. B. Sauke, R. Scholl, A. Schulte, P. J. Steinbach, J. Vittitow and R. D. Young, *Biophys. Chem.*, 1987, **26**, 337-355.
- 8 H. Frauenfelder, F. Parak and R. D. Young, *Annu. Rev. Biophys. Biophys. Chem.*, 1988, **17**, 451-479.
- 9 H. Frauenfelder, S. G. Sligar and P. G. Wolynes, *Science*, 1991, **254**, 1598-1603.
- 10 P. J. Steinbach, A. Ansari, J. Berendzen, D. Braunstein, K. Chu, B. R. Cowen, D. Ehrenstein, H. Frauenfelder, J. B. Johnson and D. C. Lamb, *Biochemistry*, 1991, **30**, 3988-4001.
- 11 G. U. Nienhaus, J. R. Mourant and H. Frauenfelder, *Proc. Natl. Acad. Sci. U.S.A.*, 1992, **89**, 2902-2906.
- 12 P. A. Cornelius, A. W. Steele, D. A. Chernoff and R. M. Hochstrasser, *Proc. Natl. Acad. Sci. U.S.A.*, 1981, **78**, 7526-7529.
- 13 E. R. Henry, J. H. Sommer, J. Hofrichter and W. A. Eaton, *J. Mol. Biol.*, 1983, **166**, 443-451.
- 14 H. Frauenfelder and P. G. Wolynes, *Science*, 1985, **229**, 337-345.
- 15 A. Ansari, C. M. Jones, E. R. Henry, J. Hofrichter and W. A. Eaton, *Science*, 1992, **256**, 1796-1798.
- 16 S. Balasubramanian, D. G. Lambright, M. C. Marden and S. G. Boxer, *Biochemistry*, 1993, **32**, 2202-2212.
- 17 D. P. Braunstein, K. Chu, K. D. Egeberg, H. Frauenfelder, J. R. Mourant, G. U. Nienhaus, P. Ormos, S. G. Sligar, B. A. Springer and R. D. Young, *Biophys. J.*, 1993, **65**, 2447-2454.
- 18 H. Li, R. Elber and J. E. Straub, *J. Biol. Chem.*, 1993, **268**, 17908-17916.
- 19 J. W. Petrich, J.-C. Lambry, S. Balasubramanian, D. G. Lambright, S. G. Boxer and J. L. Martin, *J. Mol. Biol.*, 1994, **238**, 437-444.
- 20 K. N. Walda, X. Y. Liu, V. S. Sharma and D. Magde, *Biochemistry*, 1994, **33**, 2198-2209.
- 21 S. Franzen, B. Bohn, C. Poyart and J. L. Martin, *Biochemistry*, 1995, **34**, 1224-1237.
- 22 M. Lim, T. A. Jackson and P. A. Anfinrud, *J. Biol. Inorg. Chem.*, 1997, **2**, 531-536.
- 23 Y. Kholodenko, E. A. Gooding, Y. Dou, M. Ikeda-Saito and R. M. Hochstrasser, *Biochemistry*, 1999, **38**, 5918-5924.
- 24 D. Dantsker, U. Samuni, J. M. Friedman and N. Agmon, *Biochim. Biophys. Acta, Proteins Proteomics*, 2005, **1749**, 234-251.
- 25 S. Kim, J. Heo and M. Lim, *J. Am. Chem. Soc.*, 2006, **128**, 2810-2811.
- 26 S. Kim and M. Lim, *Bull. Korean Chem. Soc.*, 2006, **27**, 1825-1831.
- 27 S. Kim and M. Lim, *Springer Ser. Chem. Phys.*, 2007, **88**, 531-533.
- 28 J. W. Petrich, J. C. Lambry, K. Kuczera, M. Karplus, C. Poyart and J. L. Martin, *Biochemistry*, 1991, **30**, 3975-3987.
- 29 O. Schaad, H. X. Zhou, A. Szabo, W. A. Eaton and E. R. Henry, *Proc. Natl. Acad. Sci. U.S.A.*, 1993, **90**, 9547-9551.
- 30 J. T. Sage, K. T. Schomacker and P. M. Champion, *J. Phys. Chem.*, 1995, **99**, 3394-3405.
- 31 A. P. Shreve, S. Franzen, M. C. Simpson and R. B. Dyer, *J. Phys. Chem. B*, 1999, **103**, 7969-7975.
- 32 D. Beece, L. Eisenstein, H. Frauenfelder, D. Good, M. C. Marden, L. Reinisch, A. H. Reynolds, L. B. Sorensen and K. T. Yue, *Biochemistry*, 1980, **19**, 5147-5157.
- 33 J. L. Martin, A. Migus, C. Poyart, Y. Lecarpentier, R. Astier and A. Antonetti, *Proc. Natl. Acad. Sci. U.S.A.*, 1983, **80**, 173-177.
- 34 J. N. Moore, P. A. Hansen and R. M. Hochstrasser, *Chem. Phys. Lett.*, 1987, **138**, 110-114.
- 35 J. W. Petrich, C. Poyart and J. L. Martin, *Biochemistry*, 1988, **27**, 4049-4060.
- 36 J. B. Miers, J. C. Postlewaite, T. Zyung, S. Chen, G. R. Roemig, X. Wen, D. D. Dlott and A. Szabo, *J. Chem. Phys.*, 1990, **93**, 8771-8776.
- 37 J. B. Miers, J. C. Postlewaite, B. R. Cowen, G. R. Roemig, I. Y. S. Lee and D. D. Dlott, *J. Chem. Phys.*, 1991, **94**, 1825-1836.
- 38 X. Ye, A. Yu, G. Y. Georgiev, F. Gruia, D. Ionascu, W. Cao, J. T. Sage and P. M. Champion, *J. Am. Chem. Soc.*, 2005, **127**, 5854-5861.
- 39 X. Ye, D. Ionascu, F. Gruia, A. Yu, A. Benabbas and P. M. Champion, *Proc. Natl. Acad. Sci. U.S.A.*, 2007, **104**, 14682-14687.
- 40 T. Lee, J. Park, J. Kim, S. Joo and M. Lim, *Bull. Korean Chem. Soc.*, 2009, **30**, 177-182.
- 41 V. Srajer, L. Reinisch and P. M. Champion, *J. Am. Chem. Soc.*, 1988, **110**, 6656-6670.
- 42 J. Park, T. Lee and M. Lim, *J. Phys. Chem. B*, 2010, **114**, 10897-10904.
- 43 X. Ye, A. Yu and P. M. Champion, *J. Am. Chem. Soc.*, 2006, **128**, 1444-1445.
- 44 J. Aron, D. A. Baldwin, H. M. Marques, J. M. Pratt and P. A. Adams, *J. Inorg. Biochem.*, 1986, **27**, 227-243.
- 45 S. Kim, G. Jin and M. Lim, *J. Phys. Chem. B*, 2004, **108**, 20366-20375.
- 46 M. Lim, M. F. Wolford, P. Hamm and R. M. Hochstrasser, *Chem. Phys. Lett.*, 1998, **290**, 355-362.
- 47 P. Hamm, M. Lim and R. M. Hochstrasser, *J. Phys. Chem. B*, 1998, **102**, 6123-6138.
- 48 P. Hamm, R. A. Kaindl and J. Stenger, *Opt. Lett.*, 2000, **25**, 1798-1800.
- 49 D. W. Urry and J. W. Pettegrew, *J. Am. Chem. Soc.*, 1967, **89**, 5276-5283.
- 50 W. I. White, *The Porphyrins*, Academic Press, New York, 1978.
- 51 W. Cao, X. Ye, G. Y. Georgiev, S. Berezina, T. Sjodin, A. A. Demidov, W. Wang, J. T. Sage and P. M. Champion, *Biochemistry*, 2004, **43**, 7017-7027.
- 52 D. R. Lide, *CRC Handbook of Chemistry and Physics*, CRC Press, Inc., Boca Raton, FL, 1995.
- 53 K. M. Hong and J. Noolandi, *J. Chem. Phys.*, 1978, **68**, 5163-5171.
- 54 F. C. Collins and G. E. Kimball, *J. Colloid Sci.*, 1949, **4**, 425-437.
- 55 D. Shoup, G. Lipari and A. Szabo, *Biophys. J.*, 1981, **36**, 697-714.
- 56 H. Kim, S. Shin and K. J. Shin, *J. Chem. Phys.*, 1998, **108**, 5861-5869.
- 57 H. Kim, *Chem. Phys. Lett.*, 2010, **484**, 358-362.
- 58 S. Kim and M. Lim, *J. Phys. Chem. B*, 2012, **116**, 5819-5830.
- 59 C. G. Malmberg, *J. Res. Natl. Bur. Stand. (U. S.)*, 1958, **60**, 609-612; Research Paper 2874.
- 60 A. Glycerine Producers, *Physical properties of glycerine and its solutions*, Glycerine Producers' Association, New York, 1963.
- 61 K. S. Cole and R. H. Cole, *J. Chem. Phys.*, 1941, **9**, 341-351.
- 62 G. E. McDuffie and T. A. Litovitz, *J. Chem. Phys.*, 1962, **37**, 1699-1705.
- 63 L. Onsager, *J. Chem. Phys.*, 1934, **2**, 599-615.
- 64 O. Chen, S. Groh, A. Liechty and D. P. Ridge, *J. Am. Chem. Soc.*, 1999, **121**, 11910-11911.

- 65 M. Meuwly, O. M. Becker, R. Stote and M. Karplus, *Biophys. Chem.*, 2002, **98**, 183-207.
- 66 G. E. McDuffie, R. G. Quinn and T. A. Litovitz, *J. Chem. Phys.*, 1962, **37**, 239-242.
- 67 S. Kim and M. Lim, *J. Am. Chem. Soc.*, 2005, **127**, 8908-8909.
- 68 S. Kim, J. Park, T. Lee and M. Lim, *J. Phys. Chem. B*, 2012, **116**, 6346-6355.
- 69 D. Ionascu, F. Gruia, X. Ye, A. Yu, F. Rosca, C. Beck, A. Demidov, J. S. Olson and P. M. Champion, *J. Am. Chem. Soc.*, 2005, **127**, 16921-16934.
- 70 P. Atkins and J. de Paula, *Atkins' Physical Chemistry, 10th Edition*, Oxford University Press, 2014.
- 71 M. J. Travers, D. C. Cowles and G. B. Ellison, *Chemical Physics Letters*, 1989, **164**, 449-455.
- 72 M. D. Bartberger, W. Liu, E. Ford, K. M. Miranda, C. Switzer, J. M. Fukuto, P. J. Farmer, D. A. Wink and K. N. Houk, *Proc. Natl. Acad. Sci. U.S.A.*, 2002, **99**, 10958-10963.
- 73 T. Prieto, R. O. Marcon, F. M. Prado, A. C. F. Caires, P. D. Mascio, S. Brochsztain, O. R. Nascimento and I. L. Nantes, *Phys. Chem. Chem. Phys.*, 2006, **8**, 1963-1973.
- 74 R. Margalit and A. Schejter, *Eur. J. Biochem.*, 1973, **32**, 492-499.
- 75 J. Kim, J. Park, T. Lee, Y. Pak and M. Lim, *J. Phys. Chem. B*, 2013, **117**, 4934-4944.
- 76 F. Schotte, J. Soman, J. S. Olson, M. Wulff and P. A. Anfinrud, *J. Structural Biol.*, 2004, **147**, 235-246.
- 77 M. Lim, T. A. Jackson and P. A. Anfinrud, *J. Chem. Phys.*, 1995, **102**, 4355-4366.
- 78 S. Kim, J. Heo and M. Lim, *Bull. Korean Chem. Soc.*, 2005, **26**, 151-156.
- 79 K. M. A. Refaey and J. L. Franklin, *Int. J. Mass Spectrom. Ion Phys.*, 1976, **20**, 19-32.
- 80 M. Cossi, V. Barone, R. Cammi and J. Tomasi, *Chem. Phys. Lett.*, 1996, **255**, 327-335.
- 81 R. Krishnan, J. S. Binkley, R. Seeger and J. A. Pople, *J. Chem. Phys.*, 1980, **72**, 650-654.
- 82 A. D. McLean and G. S. Chandler, *J. Chem. Phys.*, 1980, **72**, 5639-5648.
- 83 J. C. Rienstra-Kiracofe, G. S. Tschumper, H. F. Schaefer, S. Nandi and G. B. Ellison, *Chem. Rev.*, 2002, **102**, 231-282.
- 84 T. G. Grogan, N. Bag, T. G. Traylor and D. Magde, *J. Phys. Chem.*, 1994, **98**, 13791-13796.
- 85 K. Shikama, *Prog. Biophys. Mol. Biol.*, 2006, **91**, 83-162.
- 86 S. G. Kruglik, B.-K. Yoo, S. Franzen, M. H. Vos, J.-L. Martin and M. Negre, *Proc. Natl. Acad. Sci. U.S.A.*, 2010, **107**, 13678-13683.
- 87 S. Franzen, *Proc. Natl. Acad. Sci. U.S.A.*, 2002, **99**, 16754-16759.

TOC (2× scale)

Rebinding of NO to microperoxidase (Mp) via the harpoon mechanism.





Rebinding dynamics of NO to Microperoxidase-8 Probed by Time-resolved Vibrational Spectroscopy

Received 00th January 20xx,
Accepted 00th January 20xx

DOI: 10.1039/x0xx00000x

www.rsc.org/

Taegon Lee,^{1a} Jooyoung Kim,^{1a} Jaeheung Park,^a Youngshang Pak,^a Hyojoon Kim^{*b} and Manho Lim^{*a}

Femtosecond vibrational spectroscopy was used to probe the rebinding kinetics of NO to microperoxidase-8 (Mp), an ideal model system for the active site of ligand-binding heme proteins, including myoglobin and hemoglobin, after the photodeligation of MpNO in glycerol/water (G/W) solutions at 294 K. The geminate rebinding (GR) of NO to Mp in viscous solutions was highly efficient and ultrafast and negligibly dependent on the solution viscosity, which was adjusted by changing the glycerol content from 65% to 90% by volume in G/W mixtures. The kinetics of the GR of NO to Mp in viscous solutions was well represented by an exponential function with a time constant of ca. 11 ps. Although the kinetic traces of the GR of NO to Mp in solutions with three different viscosities (18, 81, and 252 cP) almost overlap, they show a slight difference early in the decay process. The kinetic traces were also described by the diffusion-controlled reaction theory with a Coulomb potential. Since the ligand is deligated in a neutral form, an ionic pair of NO⁻ and Mp⁺ may be produced before forming the Mp–NO bond by an electron transfer from Mp to NO as the deligated NO is sufficiently near to the Fe atom of Mp. The strong reactivity between NO and ferrous heme may arise from the Coulomb interaction between the reacting pair, which is consistent with the harpooning mechanism for NO binding to heme.

Introduction

Reaction between heme and diatomic molecules such as NO, CO, and O₂ play an important role in the physiological functions of heme proteins such as myoglobin (Mb) and hemoglobin (Hb).¹⁻⁵ Knowledge of the reactivity of these molecules with heme is essential for fully understanding the functional mechanism of heme proteins involving small gas molecules. The rebinding of diatomic molecules to heme after the photodeligation of a ligated heme protein has been intensively studied to elucidate the reactivity and reaction mechanism of heme proteins with these molecules. The rebinding kinetics of CO to Mb at cryogenic temperatures was found to be highly nonexponential and complex, which was attributed to protein conformational relaxation and/or conformational inhomogeneity.⁶⁻¹¹ The rebinding of CO and NO to Mb and Hb after photodeligation of the ligated heme proteins in solutions with various viscosities at different temperatures has also been investigated to elucidate the protein conformational relaxation and its relation to ligand binding.¹¹⁻³¹

The rebinding of ligands to heme proteins can be complicated by ligand migration within the protein and protein conformational relaxation. Comparative studies on bare heme molecules such as iron protoporphyrin IX (FePPIX) have been performed to determine the intrinsic binding characteristics of the ligand to heme in the

absence of protein environments and conformational relaxation.³²⁻⁴⁰ The kinetics of CO rebinding to H₂O-FePPIX in viscous solutions has been found to be nonexponential, even though H₂O-FePPIX has no protein environment,³⁶⁻³⁹ suggesting that the nonexponential kinetics of CO rebinding is an inherent property of bare heme. The observed nonexponential kinetics in the solvated heme was attributed to either a distribution of the rebinding barriers^{39,41} or the diffusion of the deligated CO.³⁶ In contrast to the nonexponential and temperature-dependent rebinding of CO to H₂O-FePPIX, NO rebinding to H₂O-FePPIX was observed to be exponential and independent of temperature.³⁹ Although the nonexponential rebinding of CO to bare heme was well described by the diffusive motion of the deligated CO,³⁶ the diffusion model cannot explain the exponential rebinding of NO to bare heme; as a result, the diffusion model for ligand rebinding to heme was challenged.³⁹ Alternatively, a distribution of enthalpic barriers for the rebinding has also been suggested to be responsible for the nonexponential rebinding of CO.⁴¹ However, as the diffusive ligand failed to explain the exponential rebinding kinetics of NO, the distributed enthalpic barriers could not describe the rebinding kinetics of NO to bare heme using physically meaningful parameters.⁴² A harpoon mechanism that decouples NO rebinding from the heme conformation and the diffusion of the ligand near the heme resulting from the attractive interaction between the reacting pair was suggested to describe exponential NO rebinding.⁴³

In heme proteins, the active heme is covalently bonded to a proximal histidine in its fifth coordination site, and thus, a heme molecule coordinated to a proximal histidine is better suited for the active molecule of heme proteins than H₂O-FePPIX. In this regard, microperoxidase-8 (Mp), a heme octapeptide in which a proximal histidine is covalently bonded to the heme, is an excellent model system for the active molecule of heme proteins.⁴⁴ Mp constitutes a portion of a heme protein, cytochrome c, and was prepared by the

^a Department of Chemistry and Chemistry Institute of Functional Materials, Pusan National University, Busan, 46241 Korea

^b Department of Chemistry, Dong-A University, Busan, Korea

¹ Both authors contributed equally to this work.

*To whom correspondence should be addressed.

Electronic Supplementary Information (ESI) available: [details of any supplementary information available should be included here]. See DOI: 10.1039/x0xx00000x

enzymatic digestion of cytochrome c. The rebinding of CO to Mp after the photodeligation of MpCO in solutions of various viscosities and different temperatures was measured to obtain the intrinsic reaction characteristics of CO binding to active heme in the absence of a specifically organized distal pocket and protein conformational substates.⁴² The GR of CO to Mp in viscous solutions was highly nonexponential. The GR rate and yield of CO to Mp increased with the viscosity of the solution. The viscosity-dependent kinetic behavior of CO rebinding to Mp was well reproduced by the pair survival probability function in the absence of any interaction potential between the geminate pair that was derived by the diffusion-controlled reaction model.³⁶ When the validity of the diffusion model in the absence of any interaction potential was further tested by applying the pair survival probability function to the rebinding of NO to Mp, it failed to reproduce the exponential kinetics observed in the NO rebinding.⁴² The harpoon model that successfully describes the rebinding kinetics of NO to the bare heme is based on an attractive interaction between the geminate pair. Thus, we have suggested that a diffusion model accommodating an attraction potential between the geminate pair can describe the kinetic behavior of NO rebinding.³⁶ Although the analytical form of the pair survival probability function in the presence of the interaction potential between the pair is not yet available, we were able to fit the kinetic data of NO rebinding to Mp using a pair survival probability function accommodating a Coulomb potential by numerical methods.

Here, we performed NO rebinding to Mp in solutions of three viscosities at room temperature to elucidate the reaction characteristics of NO with the active heme free from protein conformational substates and its relaxation after deligation. The GR of NO to Mp is exponential and almost independent of the viscosity of the solution used (18–252 cP). The rebinding kinetics of NO to Mp is well described by a diffusion-controlled reaction model incorporating a Coulomb potential between the geminate pair.

Materials and Methods

Femtosecond vibrational spectrometer

The details of the spectrometer are described elsewhere.⁴⁵ Briefly, a commercial Ti:sapphire regenerative amplifier (Hurricane, Spectra Physics) with a repetition rate of 1 kHz pumped by two identical home-built optical parametric amplifiers (OPA). One OPA generated a visible pump pulse at 575 nm with 3.5 μ J of energy by a frequency doubling of its signal pulse,⁴⁶ and the other OPA generated a tunable mid-IR probe pulse by difference frequency mixing of its signal and idler pulses.^{47, 48} The isotropic absorption spectrum was obtained by setting the polarization of the pump pulse at the magic angle (54.7°) relative to the probe pulse. After passing through the sample, the broadband (\sim 150 cm^{-1}) probe pulse was sent to a 320-mm monochromator with a 100-l/mm grating and then detected by a 64-element $\text{N}_2(\text{l})$ -cooled HgCdTe array detector mounted in the focal plane of the monochromator. The spectral resolution was ca. 1.6 cm^{-1} /pixel at 1660 cm^{-1} . A 12-bit analog-to-digital converter digitized the signals from each of the detector elements that were amplified with a home-built 64-channel amplifier. The pumped (A_p) and unpumped (A_u) absorbance values were obtained quasi-simultaneously by chopping the pump pulse at half the repetition frequency of the laser to calculate the pump-induced change in the absorbance of the sample ($\Delta A = A_p - A_u$). The pump-induced signal routinely exhibited less than 1.0×10^{-4} rms in absorbance units after 0.5 s of signal averaging when the IR light source was kept

stable ($<0.3\%$ rms). The probed region of the sample was uniformly photoexcited in space by keeping the pump spot sufficiently larger than the probe spot. The instrument response function was maintained at approximately 180 fs.

Sample preparation

Mp has a tendency to aggregate in solution, and the degree of aggregation is diminished by ligation, high pH, and the use of a solvent with low permittivity.^{40, 42, 44, 49-51} The MpNO sample was prepared in a glycerol/water (G/W) mixture at pH 12, and its concentration was kept low enough so that the MpNO would remain in the monomeric form.

Ferric Mp, $\text{Na}_2\text{S}_2\text{O}_4$, glycerol- d_3 , and NO gas were purchased from Sigma-Aldrich Co. and used as received. A 2-mM ferric Mp stock solution was prepared in NaOD solution and diluted with an appropriate G/W mixture. The glycerol contents in the G/W mixtures were 65, 80, and 90% by volume, which corresponded to solution viscosities of 18, 81, and 252 cP, respectively, at 294 K.⁵² The diluted ferric Mp solution was deoxygenated by bubbling with N_2 gas, reduced by adding excess amounts of $\text{Na}_2\text{S}_2\text{O}_4$ powder, and ligated with NO by bubbling the gas until the solution turned red, which is the color of MpNO. Monomeric NO-ligated Mp (MpNO) was confirmed by UV-Vis and IR spectra of the sample.^{38, 44} The final concentrations of MpNO and NaOD were 0.1 mM and 100 mM, respectively, resulting in a sample of pD = 12. The sample was passed through a gas-tight 110- μ m-path length flowing sample cell with two 2-mm-thick CaF_2 windows. The temperature of the cell was maintained at 294 ± 1 K by a circulating bath. D_2O and glycerol- d_3 were used to avoid overlap of the interested spectrum with the strong absorption bands related to the O–H moiety of the solvent.

Theory

The rebinding kinetics of CO to heme was explained by the theory of diffusion-influenced reaction in the absence of any interaction potential.^{36, 42} However, the interaction potential effects should be taken into account when considering the kinetics of NO binding to heme.⁴² The general diffusion-reaction equation for a reacting pair under the interaction potential $U(r)$ is given by⁵³

$$\frac{\partial p(r,t)}{\partial t} = D \frac{1}{r^2} \frac{\partial}{\partial r} \left(r^2 e^{-\beta U(r)} \frac{\partial}{\partial r} (e^{\beta U(r)} p(r,t)) \right) \quad (1)$$

where $p(r,t)$ is the probability distribution function at the separation r at time t and $\beta = 1/k_B T$, where k_B is the Boltzmann constant, T is the absolute temperature, and D is the relative diffusion coefficient of the reacting pair. We consider the following initial condition,

$$p(r,0 | r_0) = \frac{\delta(r-r_0)}{4\pi r_0^2} \quad (2)$$

where $\delta(r)$ is the Dirac delta function and r_0 is the initial separation between the reacting pair. The radiation boundary condition describing the reaction at encounter is given by⁵⁴

$$k_D R e^{-\beta U(r)} \frac{\partial}{\partial r} (e^{\beta U(r)} p(r,t)) \Big|_{r=R} = k_0 p(R,t) \quad (3)$$

where R is the encounter radius, k_0 is the intrinsic rate constant of reaction at R , and $k_D = 4\pi R D$ for spherically symmetric diffusion. The left-hand side represents the radial flux on the boundary surface. Here, because NO reacts only from the distal side of the heme plane, as in the previous case of CO, a reactive hemisphere is assumed, such as $k_D = 2\pi R D$.^{36, 42, 55} Once the $p(r,t)$ is calculated, the pair survival probability function, $W(t)$, can be obtained by⁵³

$$W(t) = \int_R^\infty p(r, t) dr \quad (4)$$

We assumed that the interaction potential is the Coulomb potential, $U(r) = q_1 q_2 / 4\pi\epsilon r$, where q_1 and q_2 are the charges of the reacting particles and ϵ is the permittivity of the medium. The interaction potential was represented by the Onsager length $r_c = q_1 q_2 / 4\pi\epsilon k_B T$, resulting in $\beta U(r) = r_c / r$.⁵³ The survival probability function can be obtained by solving the diffusion-reaction equation, Eq. (1), with the conditions of Eqs. (2) and (3) in the Laplace transformed domain analytically⁵³ or numerically.^{56, 57} When numerically solving a parabolic-type partial differential equation, such as Eq. (1), for a very long time, employing the fourth-order Runge-Kutta method with adaptive time-step size control and the boundary-doubling method was found to be efficient.⁵⁷

Results

Figure 1 shows the vibrational absorption of NO in MpNO in viscous solutions at 294 K. The NO absorption band was well modeled by a Gaussian function centered near 1665 cm^{-1} with 32–40 cm^{-1} FWHM (full width at half maximum). It was blue-shifted from and broader than the NO band in MbNO or HbNO.⁴⁵ The broader vibrational band for the ligand in the ligated Mp was attributed to the exposure of the ligand to inhomogeneous solvent environments compared with the well-organized protein interior in heme proteins, where the NO band has much narrower vibrational band with 9–13 cm^{-1} FWHM.^{45, 58} The NO in the aggregated MpNO likely exhibits a different stretching mode compared with the monomer, resulting in several vibrational bands in the presence of aggregated MpNO. The single-featured vibrational bands obtained using the present sample conditions indicate that the prepared sample consists of monomeric MpNO.

Figure 2 shows representative time-resolved vibrational spectra of NO in MpNO after photodeligation of the MpNO in G/W mixtures at 294 K. The shape of the transient signal does not change, but its magnitude decays with time. The negative-going feature (bleach) arises from the loss of bound NO by photodeligation, and its magnitude represents the population of the deligated Mp at the given pump-probe delay. The magnitude of the initial bleach corresponds to ca. 1% MpNO photodeligation. Only a small fraction of the sample is photoexcited because of the sample's low concentration in the short path length sample cell. This low concentration was required to maintain MpNO in the monomeric form, and the short path length was chosen to minimize the background absorption of the solvent. Most of the bleach decays within 32 ps, suggesting that the GR of the deligated NO is rapid

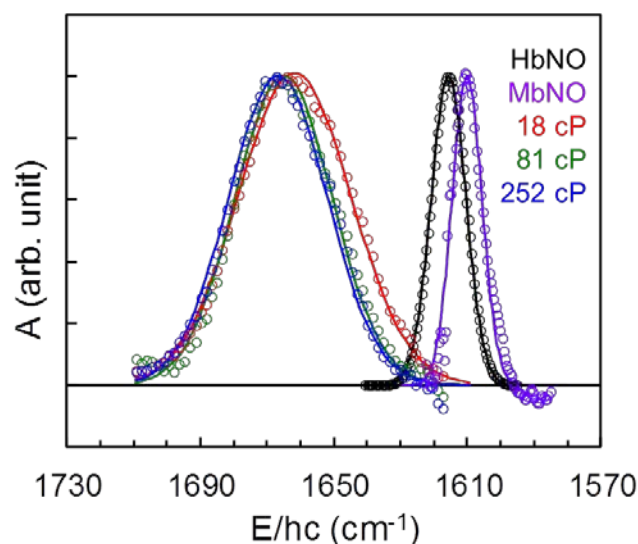


Figure 1. Equilibrium spectra of the NO stretching mode of MpNO in G/W mixtures at room temperature. The glycerol content in water was changed to vary the viscosity of the solution and was 65% (18 cP, red), 80% (81 cP, green), or 90% (252 cP, blue) by volume.⁵² Equilibrium spectra of HbNO (black) and MbNO (purple) in 70% G/W mixtures are also provided for comparison.⁵⁸ Data (open circles) were fit to a Gaussian function (solid lines).

and very efficient. The deligated Mp population was quantified by globally optimizing the entire set of spectra of a given sample using the Marquardt-Levenberg nonlinear least-squares fitting routine. An inverted Gaussian function was used to describe the bleach. Whereas the bandwidth and the center wavenumber of the Gaussian were globally optimized, the magnitude of the Gaussian was adjusted at each time point. The magnitude of the Gaussian represents the survival fraction of the deligated Mp after the photodeligation of MpNO. As shown in Figure 3, the kinetics of the magnitude decay was well described by an exponential function with a time constant of ca. 11 ps, and the time constant was nearly independent of the viscosity of the solution, indicating that the photodeligated NO geminately rebinds to Mp independently of the viscosity of the solution used.

The kinetics of NO rebinding to Mp was also fitted to the pair survival probability function derived from the diffusion-influenced bimolecular reaction in the presence of a Coulomb potential between the pair. The probability function, $W(t)$, was obtained by numerically solving Eqs. (1) and (4) using the fourth-order Runge-Kutta method with adaptive time-step size control and the boundary-doubling method.⁵⁷ The required parameters for solving

	CO			NO		
	19 cP	81 cP	252 cP	19 cP	81 cP	252 cP
R (Å)	1.36			1.36		
D (m ² /s)	5.67×10^{-11}	1.26×10^{-11}	4.04×10^{-12}	7.26×10^{-11}	1.61×10^{-11}	5.18×10^{-11}
k_0 (cm ³ /s)	4.1×10^{-14}			4×10^{-14}		
r_0 (Å)	1.53	1.51	1.48	1.50	1.45	1.41
r_c (Å)	0			55	63	70

Table 1. Parameters of the pair survival probability functions for MpCO and MpNO. The parameters for MpCO are from reference 42 and those for MpNO were obtained in this work. The encounter radius (R) was assumed to be the same as that in MpCO and the diffusion coefficient was calculated from the D value of NO in water. Three parameters (k_0 , r_0 and r_c) were obtained by fitting MpNO data in three different viscosities. The Onsager length (r_c) is zero in MpCO as no interaction potential is present.

Eq. (1) are R , D , k_0 , r_0 , and r_c . We could not fit all these parameters independently because of the finite signal-to-noise ratio of the data and the limited number of data set, and thus, we utilized the parameters obtained in a previous experiment on MpCO. The GR kinetics of CO to Mp was well reproduced by the pair survival probability function without any interaction between the pair.⁴²

Because the size of NO is almost the same as that of CO, we assumed that R is the same in both MpNO and MpCO and used the reported value for MpCO.⁴² The value of R for MpCO was obtained by fitting several experimental data of MpCO in solutions of various viscosities at 294 K and at various other temperatures (283–323 K) to the analytical expression of the pair survival probability function derived from the diffusion-controlled reaction in the absence of any interaction potential. The R value was assumed to be an intrinsic property of the CO reaction with Mp and was found to be 1.36 Å. The R value in MpCO was fitted to be independent of the solvent viscosity and temperature. Here, we also assumed that R is an intrinsic property of the NO reaction with Mp, independent of the viscosity of the solution at 294 K, and the same as the R value of MpCO (1.36 Å). Although D represents the sum of the diffusion coefficients of Mp and NO, the diffusion of Mp is negligible, and thus, D is almost the same as the diffusion coefficient of NO, as is the case in MpCO.⁴² In MpCO experiment, D was reported to be $5.67 \times 10^{-11} \text{ m}^2/\text{s}$ at 18 cP solution and related to the viscosity (η) of the solution by $D \propto 1/\eta$.⁴² The D value of NO in water is known to

be 28% larger than that of CO in water. Thus, we set the D value for MpNO to be 1.28 times that for MpCO and inversely proportional to the viscosity of the solution: $D = 7.26 \times 10^{-11} \text{ m}^2/\text{s}$ at 18 cP, $1.61 \times 10^{-11} \text{ m}^2/\text{s}$ at 81 cP, and $5.18 \times 10^{-12} \text{ m}^2/\text{s}$ at 252 cP solution. Using the fixed R and D s values, we fit data from three viscous solutions (18, 81, 252 cP) to optimize k_0 , r_0 , and r_c . In MpCO, k_0 was an intrinsic property of the reaction and independent of the viscosity of the solution. The r_0 in MpCO decreased from 1.53 to 1.51 and then to 1.45 Å as the viscosity of the solution increased from 18 to 81 and then to 252 cP. Here, we also assumed that k_0 is an intrinsic property of the NO reaction with Mp and independent of the viscosity of the solution and that r_0 is related to the solution viscosity. We optimized r_0 for the kinetic trace in a solution of 18 cP and fixed r_0 for the kinetic traces in solutions with other viscosities by scaling it to the reported r_0 of MpCO in the solution with the same viscosity. The Onsager length r_c is dependent on the permittivity of the solution, which varies with the composition of the G/W mixture. Because the permittivity of D₂O was almost the same as that of H₂O,⁵⁹ the permittivity of the G/W mixtures using deuterated solvents was considered to be approximately that of a G/W mixture without isotope substitutions, which was estimated from the experimentally available values for various G/W compositions. The estimated relative static permittivities (ϵ_{0r}) are 58, 50, and 45 for solutions with $\eta = 18, 81, \text{ and } 252 \text{ cP}$, respectively, at room temperature.⁶⁰ For monovalent ions at 294 K, the Onsager length is calculated to be 9.8 Å in 18 cP, 11.3 Å in 81 cP, and 12.5 Å in 252 cP. As the glycerol content in the G/W mixture increases, the viscosity of the solution increases, the ϵ_{0r} decreases, and the Onsager length increases, implying that the attractive interaction becomes stronger.

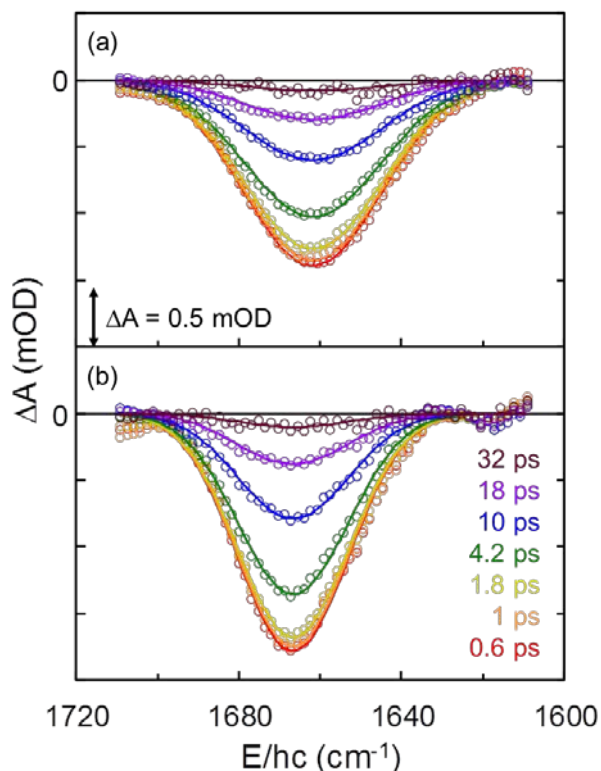


Figure 2. Representative time-resolved vibrational spectra of NO after the photodeligation of MpNO in 65% (a) and 90% (b) G/W (v/v) mixtures at 294 K. The featureless background arising from solvent absorption was modelled with a linear function and subtracted for better comparison. The remaining spectral feature (open circles) was well described by a Gaussian function (solid lines). The negative absorption arises from the loss of bound NO after photodeligation, and the magnitude of the signal is proportional to the population of the photodeligated MpNO at the given time delay. The ordinate, ΔA , is the absorption difference between the samples after and before photodeligation. The optical density (OD) unit is given in mOD ($1 \text{ mOD} = 10^{-3} \text{ OD}$) for small absorption differences. The pump-probe delays are 0.6, 1, 1.8, 4.2, 10, 18, and 32 ps (bottom to top) and are colour coded.

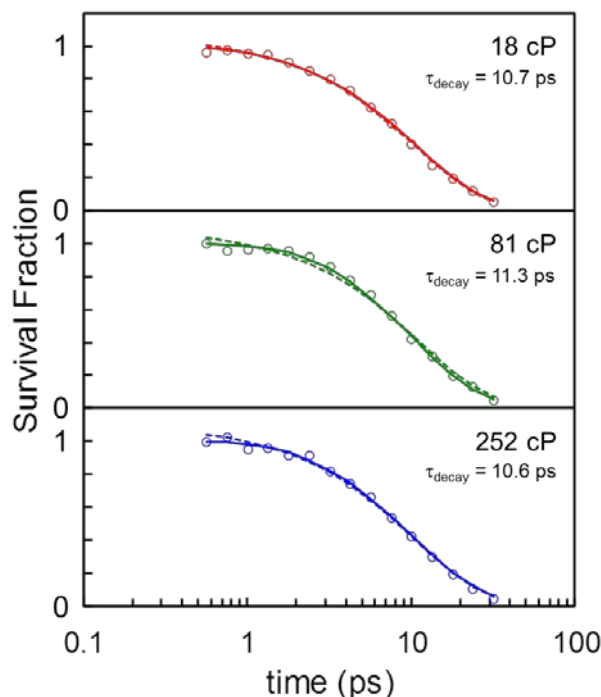


Figure 3. Kinetics of survival fraction of deligated heme after photodeligation of MpNO in the 18 cP (red), 81 cP (green), and 252 cP (blue) solutions at 294 K. The kinetic data (open circles) were fit to an exponential function with time constants of about 11 ps (dashed lines) as well as the theory of diffusion-controlled reaction in the presence of a Coulomb attractive potential (solid lines).

As mentioned previously, 5 parameters (R , D , k_0 , r_0 , and r_c) were required to calculate $W(t)$, and these 5 parameters were globally applied to fit all of the decay kinetics in solutions with various viscosities. The values for R and k_0 are the same for all the kinetic traces. Although the values for D , r_0 , and r_c were global, D and r_0 varied with the viscosity and r_c varied with the permittivity of the solution. First, we related the R and D values to the previous fitting of MpCO and fixed them. Then, we optimized the remaining three parameters to fit all the kinetic traces of MpNO. The best fitting values were $k_0 = 4 \times 10^{-14} \text{ cm}^3/\text{s}$, $r_0 = 1.5 \text{ \AA}$, and $r_c = 55 \text{ \AA}$ for the 18-cP solution (see Table 1). Except k_0 , r_0 and r_c varied with the viscosity of the solution and exhibited values of 1.41 and 70 \AA , respectively, in the 252-cP solution. A much larger r_c was needed to fit the data than the value calculated using ϵ_{or} . However, since the permittivity depends on the frequency of the applied electric field, and the permittivities of water and glycerol at high frequencies can be 1/45 and 1/12 of the static value, respectively,^{61, 62} the fitted Onsager length, which required the relative permittivity (ϵ_r) to be $\epsilon_r = \epsilon_{\text{or}} / 5.6$, is certainly feasible (see the Discussion section).

Considering that only three global parameters (k_0 , r_0 and r_c) were adjusted to fit all three kinetics traces, the consistency between the experimental GR kinetic data and the theoretical predictions is remarkable (see Figure 3). For a higher viscosity solution, the diffusive encounter occurs more slowly, but the shorter initial separation and the stronger attraction field cause the reactions to occur more rapidly. Because these effects are contradictory, the survival probability curves do not show much difference, unlike those in the case of CO without an interaction potential. Note that the attraction field effect dominates the long-term kinetics, namely, $S(\infty) \approx \exp(-r_c/r_0)$, as predicted by Onsager,⁶³ while this relation was $S(\infty) = 1 - \frac{R}{r_0} \frac{k_0}{k_D + k_0}$ for CO. $S(\infty)$ represents the fraction of the escaped ligand without GR after photodeligation of the ligated molecule. Because $r_c/r_0 \gg 1$ for the reaction of NO with Mp, the escaped fraction of NO without GR after the photodeligation of MpNO is negligible, as was observed. For MpCO, where there is no interaction potential between Mp and CO, a large fraction of the photodeligated CO escapes without GR. Therefore, Figure 3 clearly demonstrates the existence of a strong attraction field between Mp and NO.

Discussion

Because the heme was excited by a 575-nm photon, the energy of which (208 kJ/mol) is much larger than the bond energy of the Fe–NO of heme (113–125 kJ/mol),^{64, 65} the excess energy should be distributed into Mp and the deligated NO upon photolysis of MpNO. The energy in the NO will be distributed amongst its vibrational, rotational, and translational motions, and thus, when more energy is deposited into the vibrational or rotational motion of the deligated NO, it will have less translational energy. The NO with excess translational energy will fly off the Mp upon the photodeligation of MpNO. A molecular dynamics (MD) simulation has shown that the photodeligated NO from MbMO with excess kinetic energy is thermalized within 0.3 ps and that its motion subsequently becomes diffusive.⁶⁵ Therefore, the detached NO likely exhibits diffusive thermal motion shortly after

photodeligation, even if it has flown off of Mp because of excess kinetic energy. In the MpCO experiment, diffusive motion well described the behavior of the photodeligated ligand that flew off because of excess kinetic energy. The photodetached ligand that flew off achieved greater initial separations in less viscous solutions. If there is no attractive interaction between NO and Mp, the diffusive NO will drift away from the Mp, and in less viscous solutions, the diffusion will be more rapid, resulting in slower, less frequent GR, as observed in the GR kinetics of MpCO. However, although the initial separation and diffusion rate depend on the viscosity of the solution, the GR kinetics of NO to Mp in various viscous solutions converges as time passes (see Figure 4), indicating that GR is dictated not by the diffusive motion but instead by the attractive interaction. We calculated the GR kinetics of NO to Mp when there is no attractive interaction between NO and Mp by setting $r_c = 0$ and keeping all other parameters the same. As can be seen in Figure 4, the calculated GR kinetics with $r_c = 0$ (the dotted lines) heavily depends on the viscosity of the solution, more NO rebinds faster in more viscous solution, which is consistent with the observed GR kinetics of CO to Mp⁴² but inconsistent with the experimental GR kinetics of NO to Mp.

The fitted Onsager lengths of 55–70 \AA are 5.6 times larger than the calculated values of 9.8–12.5 \AA using static permittivity. As mentioned previously, the permittivity depends on the frequency of the applied electric field. Since the photodeligated ligand from MpNO is a neutral NO (*vide infra*), the reacting pair (Mp, NO) experiences the Coulombic interaction only after a charged pair is formed. A charged pair can be formed by an electron transfer from Mp to NO. The permittivity can be conceived of as the ability to diminish the Coulomb interaction between charged compounds by rearranging the charge distribution of the surrounding solvent molecules. When the charged pair is formed after an electron transfer, the static permittivity is not appropriate for calculating the immediate Coulomb interaction between the newly formed charged pair. Because the GR time constant of NO to Mp is approximately 11 ps, the electron transfer should occur earlier than

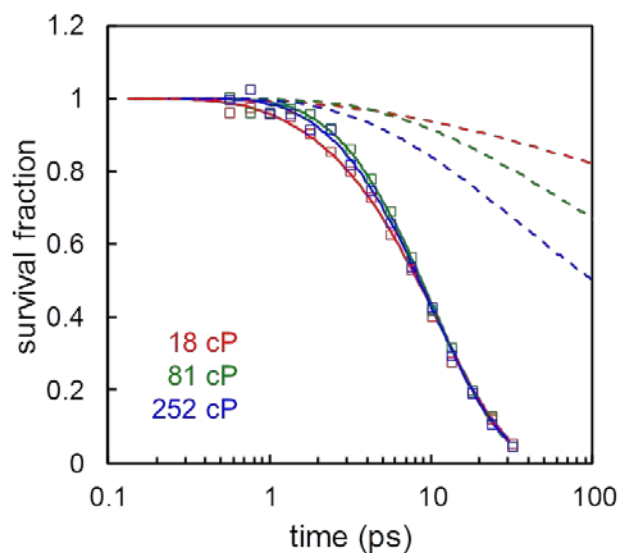


Figure 4. Simulated kinetics of the survival fraction of deligated heme after the photodeligation of MpNO in 18-cP (red), 81-cP (green), and 252-cP (blue) solutions when the Coulomb attraction was removed by setting $r_c = 0$ (dashed lines) while keeping all other parameters equal to the best fit. When the Coulomb interaction is absent, the GR of the deligated NO to Mp becomes slower, and its kinetics depends on the viscosity of the solution, as observed for the GR of CO to Mp. For comparison, GR kinetic data (open squares) of NO to Mp are also shown with their best fits (solid lines).

11 ps, as if the electric field is produced at a frequency exceeding 91 GHz. Using the reported frequency-dependent permittivities of G/W mixtures at 265.5 K,⁶⁶ the ϵ_r values of 82% and 90% G/W (v/v) mixtures at 265.5 K are calculated to be 4.3 and 4.1 at 100 GHz, respectively; furthermore, both of these values approach the asymptotic value of 4 at 1000 GHz. Based on the temperature-dependent permittivity of glycerol,⁶² the ϵ_r values of glycerol at 265 K and 285 K are calculated to be 4.7 and 5.3 at 2 GHz; both reach 4.1 at 100 GHz and approach 4 at 1000 GHz. The permittivity of G/W mixtures quickly approaches the value of pure glycerol as the frequency or the glycerol content increases.⁶⁶ Although the frequency-dependent ϵ_r values of G/W mixtures at 294 K are not available, we were able to estimate them by extrapolating the parameters to calculate the frequency-dependent permittivity from the reported experimental measurements.^{62, 66} The estimated ϵ_r value for the Mp + NO reaction in G/W mixtures could be as small as 4.6–4.1, lower than the static value of 58–45. Clearly, the Onsager length can be as large as 11 times the calculated r_c using the static permittivity. Thus, the fitted r_c value, which requires ϵ_r to be 10.4–8, is certainly within the range of the feasible permittivity of the G/W mixture. The GR kinetic data of NO to Mp were also reproduced when fitted by fixing r_c to the calculated value using $\epsilon_r = 4.6$ –4.1 by adjusting only k_0 to be $1.8 \times 10^{-14} \text{ cm}^3/\text{s}$.

Although an attractive interaction between NO and Mp is crucial to explain the observed GR kinetics of NO to Mp, the MpNO does not appear to photodissociate into ionic species, i.e., NO^- and Mp^+ . When MbNO or HbNO was photoexcited with a 575-nm photon, the neutral ligand NO, not NO^- , has been directly observed.^{58, 67, 68} When H_2O -FePPIX-NO or MbNO was photoexcited by a 580-nm photon, ferrous heme, not ferric heme, has been shown to appear immediately upon photodeligation.⁶⁹ Therefore, MpNO should photodissociate into the neutral species NO and Mp. A neutral pair can attract each other when an electron from one molecule is transferred to the reacting partner, thus generating an ionic pair before the bond is formed. The textbook description of the harpoon mechanism underlying the gas-phase reaction indicates that an electron can be transferred from a molecule (donor) to the reacting partner (acceptor) if the distance between the reacting pair is within the harpoon distance (r_H) defined by $IE - EA - e_2/4\pi\epsilon_0 r_H < 0$, where ϵ_0 is the permittivity of the vacuum and e is the electronic charge.⁷⁰ Here, IE and EA represent the ionization energy of the donor and the electron affinity of the acceptor compound, respectively. In the solution phase, we may define the r_H that satisfies the equation $\Delta G_{\text{acceptor}}^{\circ} + \Delta G_{\text{donor}}^{\circ} - e_2/4\pi\epsilon_r r_H < 0$, where $\Delta G_{\text{acceptor}}^{\circ}$ and $\Delta G_{\text{donor}}^{\circ}$ are the standard reaction Gibbs energies of the half reactions to accept and donate an electron, respectively.

In the case of MpNO in G/W mixtures, $\Delta G_{\text{acceptor}}^{\circ}$ and $\Delta G_{\text{donor}}^{\circ}$ are the standard reaction Gibbs energies of $\text{NO} + e^- \rightarrow \text{NO}^-$ and $\text{Mp} \rightarrow \text{Mp}^+ + e^-$ in solution, respectively, when each compound is at a concentration of 1 M. These values are simply related to the standard reduction potentials of NO and Mp^+ as follows,

$$\Delta G_{\text{acceptor}}^{\circ} = -FE^{\circ}(\text{NO}/\text{NO}^-)$$

$$\Delta G_{\text{donor}}^{\circ} = FE^{\circ}(\text{Mp}^+/\text{Mp}),$$

where F is the Faraday constant and $E^{\circ}(\text{NO}/\text{NO}^-)$ and $E^{\circ}(\text{Mp}^+/\text{Mp})$ are the standard reduction potentials of NO and Mp^+ , respectively, when all the compounds are at concentrations of

1 M. Therefore, the reduction potential was given for 1 M of compounds versus normal hydrogen electrode hereafter. EA of NO has a slightly positive value of 0.026 eV,⁷¹ but $E^{\circ}(\text{NO}/\text{NO}^-)$ has a negative value of -0.8 V ,⁷² suggesting that the reduction of NO is spontaneous in the gas phase but nonspontaneous in solution. $E^{\circ}(\text{Mp}^+/\text{Mp})$ was reported to be 0.34 V at pH = 7.4,⁷³ but it is not known at pH = 12, which was the pH used here. Similar to Mp^+ , the reduction potential of ferric cytochrome c was found to decrease as the pH of the solution increased and is near zero when the solution pH = 12.⁷⁴ Thus, $E^{\circ}(\text{Mp}^+/\text{Mp})$ should be smaller than 0.34 V and could be near zero at pH = 12. For the reaction of $\text{Mp} + \text{NO} \rightarrow \text{Mp}^+ + \text{NO}^-$ in solution, $\Delta G_{\text{acceptor}}^{\circ} + \Delta G_{\text{donor}}^{\circ}$ were calculated to be 77–110 kJ/mol using the reported reduction potentials of $E^{\circ}(\text{NO}/\text{NO}^-) = -0.8 \text{ V}$ and $0 \text{ V} \leq E^{\circ}(\text{Mp}^+/\text{Mp}) < 0.34 \text{ V}$, resulting in $r_H = 3.1$ –4.4 Å in $\epsilon_r = 4.1$ solution and $r_H = 1.3$ –1.8 Å in $\epsilon_r = 10$ solution. As long as the solution has $\epsilon_r < 8.4$, the harpoon mechanism can function in the Mp–NO bond formation because r_H exceeds 1.5 Å (the largest initial separation in MpNO) when $\epsilon_r < 8.4$. As discussed previously, $\epsilon_r < 8.4$ is within the feasible ϵ_r range of the G/W mixtures used here when the dynamics nature of the induced electric field is taken into account. Although the reduction of NO is unfavorable in solution, the GR kinetics of NO to Mp indicates that an electron of Mp can be transferred to NO within the harpoon distance, producing the ionic reacting pair, Mp^+ and NO^- , before forming the Mp–NO bond. Because NO^- is readily formed in the gas phase (as can be seen from the positive value of EA for NO), the electron transfer from Mp to the geminate NO appears to be both kinetically and thermodynamically feasible.

The GR process following the photodeligation is highly nonequilibrium process but we calculated the energetics of the electron transfer from Mp to NO using the equilibrium Gibbs energy. Furthermore, the positive charge in Mp might be delocalized over the heme. Thus the calculated energetics is a rough estimate for the electron transfer. However, it may be the only way to check the energetic feasibility of the electron transfer without running atomistic MD simulation. Atomistic MD simulations may show the nonequilibrium energetics as well as the detailed charge distribution in the heme needed to estimate the realistic energetics for the electron transfer.

NO is deligated in a neutral form and the fast rebinding of NO to Mp was well described by the diffusion-controlled reaction theory in the presence of a Coulomb potential. The electron transfer from Mp to NO appears to be feasible energetically as long as the reacting pair are within the harpoon distance, which can be as large as 4 Å. Thus the deligated NO diffuses around in a neutral form before an electron is transferred from Mp to NO, producing ionic pair (Mp^+ and NO^-). Once the ionic pair is formed, the Coulombic attraction between two ions starts to dominate and induces a rapid formation of the Fe–NO bond. Clearly, if happens, the electron transfer precedes the formation of the bond. We have shown that the electron transfer is feasible thermodynamically but the time constant for the electron transfer, which should be smaller than 11 ps, is not recovered in the present model.

In the diffusion-controlled reaction theory with a Coulomb potential, the reacting pair is charged all the time during diffusion. However, the deligated ligand from MpNO is the neutral NO and is charged by an electron transfer when it is within the harpoon distance from Mp. Therefore, more realistic model for the GR of NO to Mp may be the diffusion-controlled reaction theory with a Coulomb potential that is turned on with a certain time constant.

Before such a model is available, the fitted parameters obtained here can be used as a rough estimate for the corresponding parameters.

When the NO^- and Mp^+ are formed during the rebinding, can their spectroscopic features be observed? With the time-resolved IR spectroscopy, we see the spectroscopic feature when a measurable fraction of a compound is accumulated at some point in time.⁷⁵ When population of an intermediate is sufficient to be observed at a given time, its spectroscopic marker will show up.⁷⁶ Vibrational spectrum of NO^- can be observed only when the NO^- either forms simultaneously in a sufficient quantity or is accumulated enough at a given time. As discussed, the NO diffuses around in a neutral form and becomes NO^- via electron transfer before forming the Mp-NO bond. Since the NO^- forms asynchronously and the produced NO^- disappears quickly due to the MpNO formation, NO^- cannot be accumulated in a sufficient quantity to be observable and thus, its vibrational spectrum is unlikely detectable. Even the population of NO^- is accumulated enough at some point in time, its vibrational band is observable only when its absorptivity of NO^- is large enough to be detected. The absorptivity of the vibrational band of NO^- is not known but that of NO is about 30 times smaller than that of NO^- bound to heme.⁵⁸ The vibrational band of the deligated NO in solution has not been detected yet due to low absorptivity and possibly broad band width. If the absorptivity of the vibrational band of NO^- is similar to that of the deligated NO, even all the deligated ligand becomes NO^- , the magnitude of the vibrational spectrum of NO^- is too small to be detected in our experimental conditions.

As mentioned previously, the photodeligated NO will fly off from Mp, and its motion will become diffusive rapidly because of collisions with the surrounding solvent molecules. We defined the initial separation to be the distance at which the photodeligated NO loses its excess translational energy and begins to exhibit diffusive motion. As the kinetic energy of the detached NO increases, the initial separation from Mp increases, and r_0 thus also increases. Because there will be a distribution of initial separation, the value of r_0 represents an average of the initial separations achieved by NO after photodeligation. The initial separation of the photodeligated NO from MpNO ranges from 1.5 to 1.41 Å, which is slightly smaller than that of the photodeligated CO from MpCO (1.53–1.45 Å). This range is consistent with the reported population of the vibrationally excited ligand after the photolysis of ligated Mb, a similar heme system. When MbNO and MbCO were photoexcited by a 575-nm photon, approximately 15% of NO^{67} and 6% of $\text{CO}^{77,78}$ respectively, were deligated in the vibrationally excited state. When the same energy is deposited into the deligated ligand, as more energy is partitioned into its vibrational energy, less energy will be partitioned into its translational energy, resulting in a smaller initial separation. Because more NO than CO is vibrationally excited when detached from heme, a greater proportion of NO will likely exhibit less excess kinetic energy as long as the similar amount of energy is deposited into the deligated ligand and thus achieve shorter average separations after thermalization.

The value for the encounter radius, $R = 1.36$ Å, which we assumed to be the same as in MpCO , is even shorter than the Fe–N bond length of 1.74 Å.⁶⁵ The encounter radius should be at least the distance between the Fe and the center of the NO molecule. The NO molecule should both have the appropriate orientation to form the Fe–NO bond and be within reacting distance. The fitted encounter radius was underestimated because some NO molecules within the bonding distance cannot bind to Mp because of

improper orientation. Thus, the value for the encounter radius, 1.36 Å represents a value at least 1.74 Å in reality. In the same logic, the fitted initial separation should be larger than 1.74 Å. Using a simple scaling, r_0 of 1.5 ~ 1.41 Å represents the value of at least 1.92 ~ 1.8 Å, suggesting that the initial separation of the deligated NO is about 2 Å from the Fe. The intrinsic rate constant at the encounter distance of NO and Mp is almost equivalent to or smaller than that of CO and Mp, suggesting that the more rapid GR of NO to Mp is not attributable to the more rapid intrinsic rate constant but is instead due to the attractive interaction resulting from the electron transfer that occurs before bond formation.

As mentioned previously, the deligated NO can be charged by an electron transfer from Mp when the initial separation between Mp and NO is shorter than the harpoon distance. However, if the initial separation is large enough to prohibit the electron transfer, the NO will diffuse away, and GR will become less efficient. A large initial separation is expected in low viscosity solutions. Our preliminary data on NO rebinding to Mp in methanol ($\eta = 0.544$ cP) showed that approximately 70% of the deligated NO geminately rebound with a time constant of ca. 7 ps and that the remainder escaped without GR. This observation indicates that a portion of the deligated ligand achieved a sufficient initial separation to prevent the occurrence of electron transfer in low viscosity solution. The neutral ligand exhibits purely diffusive motion and drifts away from Mp. As observed in the MpCO experiment, the deligated ligand did not geminately rebound to any extent in low viscosity solution because of its rapid diffusion away from Mp.⁴²

Whereas the deligated NO can geminately rebound to Mp in an ionic form under the influence of Coulomb attraction because of the transfer of an electron from Mp to NO before the formation of the Mp-NO bond, the deligated CO geminately rebounds to Mp through pure diffusion of the neutral CO. Why can NO generate an ionic pair with Mp before forming the bond but CO cannot? The reduction potential of NO was calculated from its EA and the solvation energies of NO^- and NO using the known reduction potential of O_2 as a reference value.⁷² The reduction potential of CO , $E^\circ(\text{CO}/\text{CO}^-)$, which is not known, was estimated from its EA (-1.326 eV)⁷⁹ and the solvation energies of CO^- and CO using $E^\circ(\text{NO}/\text{NO}^-)$ as a reference value. The solvation energies of CO^- and CO, which were calculated using the polarizable continuum model⁸⁰ by B3LYP with the 6-311+G* basis set^{81,82} in G/W mixtures, were 25–33 kJ/mol higher than those of NO^- and NO. Thus, $E^\circ(\text{CO}/\text{CO}^-)$ was estimated to be a larger negative value than -2.4 V. Using the estimated $E^\circ(\text{CO}/\text{CO}^-)$, $\Delta G_{\text{acceptor}}^\circ + \Delta G_{\text{donor}}^\circ$ for the reaction of $\text{Mp} + \text{CO} \rightarrow \text{Mp}^+ + \text{CO}^-$ in solution was calculated to be larger than 231 kJ/mol, and therefore, $r_H < 1.46$ Å in $\epsilon_r = 4.1$ solution and $r_H < 0.6$ Å in $\epsilon_r = 10$ solution. Because the initial separation between Mp and CO exceeds 1.45 Å, the electron transfer from Mp to CO is thermodynamically unfavorable. Furthermore, highly unstable gas-phase CO^- may also kinetically hinder the formation of CO^- . In contrast to NO^- , the formation of CO^- appears to be both kinetically and thermodynamically unfavorable, which is likely the underlying reason for the purely diffusional rebinding of CO to Mp.

The reduction potential of O_2 is -0.16 V,⁷² implying that, although unfavorable, O_2^- can be much more readily formed in solution than NO^- . Because the EA of O_2 exhibits a positive value of 0.451 eV,⁸³ O_2^- is highly favorable in the gas phase. Thus, an electron transfer from Mp to O_2 in solution is certainly kinetically

and thermodynamically feasible. As long as the separation between the neutral Mp and O₂ is sufficiently small, an electron can be transferred from Mp to O₂, resulting in an ionic pair of Mp⁺ and O₂⁻. Once the ionic pair is produced, the GR kinetics of O₂ to Mp would be as rapid and efficient as that of NO to Mp. However, if the initial separation is large because of the low viscosity of the solution and the electron transfer is thus kinetically prohibited, the deligated O₂ will diffuse away without GR. According to the GR kinetics of O₂ to picket fence heme in toluene ($\eta = 0.59$), only a fraction of the deligated O₂ geminately rebinds, and the GR kinetics occurs on the picosecond time scale.⁸⁴ Clearly, the GR of O₂ to heme can be described by the reaction between the charged pair generated by an electron transfer from the heme to O₂ when they are sufficiently close. In fact, because O₂⁻ readily forms in solution because of the low reduction potential of O₂, O₂-ligated heme is relatively unstable.⁸⁵ For example, Mp⁺ + O₂⁻ in solution can be more stable than MpO₂ if Mp⁺ is stabilized by an interaction, such as the coordination of water to Mp⁺. Indeed, when MpO₂ sample preparation was attempted by adding O₂ to Mp, oxidized heme (Mp⁺) was formed instead of MpO₂. O₂-ligated hemes, such as oxy heme proteins and picket fence heme, can be formed when they are stabilized by blocking the attack of nucleophilic species or forming a hydrogen bond with a side chain.^{84, 85}

To test the validity of the $W(t)$, the pair survival probability function derived from the diffusion-influenced bimolecular reaction with a Coulomb interaction used to describe the GR kinetics of NO to heme, we simulated the GR kinetics of NO to H₂O-FePPIX in the temperature range of 290–200 K and observed exponential and almost temperature-independent kinetics (Figure 1B in Ye et al.³⁹). During the simulation, R and k_0 were set to be the same as the best fitted parameters for MpNO in solutions of various viscosities at 294 K. Additionally, r_0 and D were scaled to the viscosity of the solution, and r_c was adjusted for the permittivity of the solution and temperature. As can be seen in Figure 5, the simulated data reasonably reproduce the experimental observation that GR kinetics is exponential and almost independent of temperature, which supports the validity of the model and fitted parameters. Because k_0 was found to depend on temperature in the GR of CO to H₂O-FePPIX, a better simulation can be obtained by adjusting k_0 .

Although the harpoon mechanism well describes the kinetics of NO rebinding to Mp, it might be a specific property of Mp reacting with NO. More works are required to generalize the harpoon mechanism to the reaction of NO with Mb and Hb.

Fast and exponential rebinding of NO to a model heme was suggested to arise from the bonding of NO to the domed heme.⁶⁹ Binding of NO to the domed heme was observed in various heme proteins.⁸⁶ The binding of NO to the domed heme was attributed to the electronic property of NO such that it has an unpaired electron, which enables NO to form a bond with the electron in the d_{z^2} orbital of high-spin Fe(II) atom in the domed heme.⁶⁹ It was consistent with a density functional theory calculation showing that the intermediate spin state of NO is a bound state.⁸⁷ Although the kinetics of NO rebinding to Mp is well described by the diffusion-controlled reaction with a Coulomb potential and the electron transfer from Mp to NO is thermodynamically feasible, there is no direct evidence for the formation of the ionic pair (Mp⁺, NO⁻). Thus, the Coulomb attraction in the diffusion model may be not due to the formation of the ionic pair but simply reflect the electronic property of NO leading to its fast binding to the domed heme.

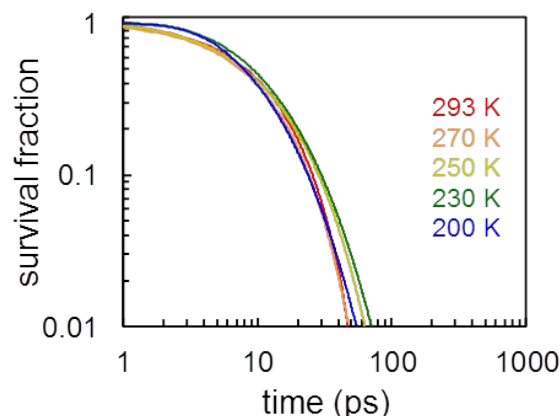


Figure 3 Simulated kinetics of NO rebinding to H₂O-FePPIX at 290 (red), 270 (orange), 250 (pink), 230 (green), and 200 K (brown). The pair survival probability function, $W(t)$, was calculated by properly adjusting the best fitted parameters for MpNO at 294 K; R and k_0 were kept the same, r_0 and D were scaled to the viscosity of the solution, and r_c was adjusted for the permittivity of the solution and temperature.

Conclusions

NO rebinding kinetics with Mp after the photodeligation of MpNO in three viscous solutions was investigated at 294 K using femtosecond infrared spectroscopy. The GR of photodeligated NO to Mp is ultrafast, highly efficient, and almost independent of the viscosity of the solution. Most of the photodeligated NO geminately rebinds to Mp with a time constant of ca. 11 ps, and the geminate yield is near unity. The GR kinetics was well described by the diffusion-influenced bimolecular reaction in the presence of a Coulomb potential between the reacting pair. When MpNO is photoexcited, the ligand is detached in a neutral form, but an electron can be transferred from Mp to NO when they are within the harpoon distance, producing the ionic pair, Mp⁺ and NO⁻, before the Mp-NO bond forms. The Coulomb attraction between the ionic pair may be responsible for the rapid and efficient GR of NO to Mp. The viscosity-independent GR kinetics of NO to Mp indicates that the Coulomb attraction dominates the diffusional motion of the deligated NO.

Acknowledgements

This work was supported by the National Research Foundation of Korea (NRF) grant funded by the Korea government (MEST) (NRF-2014R1A2A2A01002456, NRF-2014R1A4A1001690). J. Kim was supported by the 2014 Post-Doc Development Program of Pusan National University.

References

- 1 E. Antonini and M. Brunori, *Hemoglobin and Myoglobin in Their Reactions With Ligands*, North-Holland Publishing Company, London, UK, 1971.
- 2 L. Jia, C. Bonaventura, J. Bonaventura and J. S. Stamler, *Nature*, 1996, **380**, 221-226.

- 3 S. Moncada and A. Higgs, *N. Engl. J. Med.*, 1993, **329**, 2002-2012.
- 4 C. Nathan, *FASEB Journal*, 1992, **6**, 3051-3064.
- 5 J. S. Stamler, D. J. Singel and J. Loscalzo, *Science*, 1992, **258**, 1898-1902.
- 6 R. H. Austin, K. W. Beeson, L. Eisenstein, H. Frauenfelder and I. C. Gunsalus, *Biochemistry*, 1975, **14**, 5355-5373.
- 7 A. Ansari, J. Berendzen, D. K. Braunstein, B. R. Cowen, H. Frauenfelder, M. K. Hong, I. E. T. Iben, J. B. Johnson, P. Ormos, T. B. Sauke, R. Scholl, A. Schulte, P. J. Steinbach, J. Vittitow and R. D. Young, *Biophys. Chem.*, 1987, **26**, 337-355.
- 8 H. Frauenfelder, F. Parak and R. D. Young, *Annu. Rev. Biophys. Biophys. Chem.*, 1988, **17**, 451-479.
- 9 H. Frauenfelder, S. G. Sligar and P. G. Wolynes, *Science*, 1991, **254**, 1598-1603.
- 10 P. J. Steinbach, A. Ansari, J. Berendzen, D. Braunstein, K. Chu, B. R. Cowen, D. Ehrenstein, H. Frauenfelder, J. B. Johnson and D. C. Lamb, *Biochemistry*, 1991, **30**, 3988-4001.
- 11 G. U. Nienhaus, J. R. Mourant and H. Frauenfelder, *Proc. Natl. Acad. Sci. U.S.A.*, 1992, **89**, 2902-2906.
- 12 P. A. Cornelius, A. W. Steele, D. A. Chernoff and R. M. Hochstrasser, *Proc. Natl. Acad. Sci. U.S.A.*, 1981, **78**, 7526-7529.
- 13 E. R. Henry, J. H. Sommer, J. Hofrichter and W. A. Eaton, *J. Mol. Biol.*, 1983, **166**, 443-451.
- 14 H. Frauenfelder and P. G. Wolynes, *Science*, 1985, **229**, 337-345.
- 15 A. Ansari, C. M. Jones, E. R. Henry, J. Hofrichter and W. A. Eaton, *Science*, 1992, **256**, 1796-1798.
- 16 S. Balasubramanian, D. G. Lambright, M. C. Marden and S. G. Boxer, *Biochemistry*, 1993, **32**, 2202-2212.
- 17 D. P. Braunstein, K. Chu, K. D. Egeberg, H. Frauenfelder, J. R. Mourant, G. U. Nienhaus, P. Ormos, S. G. Sligar, B. A. Springer and R. D. Young, *Biophys. J.*, 1993, **65**, 2447-2454.
- 18 H. Li, R. Elber and J. E. Straub, *J. Biol. Chem.*, 1993, **268**, 17908-17916.
- 19 J. W. Petrich, J.-C. Lambry, S. Balasubramanian, D. G. Lambright, S. G. Boxer and J. L. Martin, *J. Mol. Biol.*, 1994, **238**, 437-444.
- 20 K. N. Walda, X. Y. Liu, V. S. Sharma and D. Magde, *Biochemistry*, 1994, **33**, 2198-2209.
- 21 S. Franzen, B. Bohn, C. Poyart and J. L. Martin, *Biochemistry*, 1995, **34**, 1224-1237.
- 22 M. Lim, T. A. Jackson and P. A. Anfinrud, *J. Biol. Inorg. Chem.*, 1997, **2**, 531-536.
- 23 Y. Kholodenko, E. A. Gooding, Y. Dou, M. Ikeda-Saito and R. M. Hochstrasser, *Biochemistry*, 1999, **38**, 5918-5924.
- 24 D. Dantsker, U. Samuni, J. M. Friedman and N. Agmon, *Biochim. Biophys. Acta, Proteins Proteomics*, 2005, **1749**, 234-251.
- 25 S. Kim, J. Heo and M. Lim, *J. Am. Chem. Soc.*, 2006, **128**, 2810-2811.
- 26 S. Kim and M. Lim, *Bull. Korean Chem. Soc.*, 2006, **27**, 1825-1831.
- 27 S. Kim and M. Lim, *Springer Ser. Chem. Phys.*, 2007, **88**, 531-533.
- 28 J. W. Petrich, J. C. Lambry, K. Kuczera, M. Karplus, C. Poyart and J. L. Martin, *Biochemistry*, 1991, **30**, 3975-3987.
- 29 O. Schaad, H. X. Zhou, A. Szabo, W. A. Eaton and E. R. Henry, *Proc. Natl. Acad. Sci. U.S.A.*, 1993, **90**, 9547-9551.
- 30 J. T. Sage, K. T. Schomacker and P. M. Champion, *J. Phys. Chem.*, 1995, **99**, 3394-3405.
- 31 A. P. Shreve, S. Franzen, M. C. Simpson and R. B. Dyer, *J. Phys. Chem. B*, 1999, **103**, 7969-7975.
- 32 D. Beece, L. Eisenstein, H. Frauenfelder, D. Good, M. C. Marden, L. Reinisch, A. H. Reynolds, L. B. Sorensen and K. T. Yue, *Biochemistry*, 1980, **19**, 5147-5157.
- 33 J. L. Martin, A. Migus, C. Poyart, Y. Lecarpentier, R. Astier and A. Antonetti, *Proc. Natl. Acad. Sci. U.S.A.*, 1983, **80**, 173-177.
- 34 J. N. Moore, P. A. Hansen and R. M. Hochstrasser, *Chem. Phys. Lett.*, 1987, **138**, 110-114.
- 35 J. W. Petrich, C. Poyart and J. L. Martin, *Biochemistry*, 1988, **27**, 4049-4060.
- 36 J. B. Miers, J. C. Postlewaite, T. Zyung, S. Chen, G. R. Roemig, X. Wen, D. D. Dlott and A. Szabo, *J. Chem. Phys.*, 1990, **93**, 8771-8776.
- 37 J. B. Miers, J. C. Postlewaite, B. R. Cowen, G. R. Roemig, I. Y. S. Lee and D. D. Dlott, *J. Chem. Phys.*, 1991, **94**, 1825-1836.
- 38 X. Ye, A. Yu, G. Y. Georgiev, F. Gruia, D. Ionascu, W. Cao, J. T. Sage and P. M. Champion, *J. Am. Chem. Soc.*, 2005, **127**, 5854-5861.
- 39 X. Ye, D. Ionascu, F. Gruia, A. Yu, A. Benabbas and P. M. Champion, *Proc. Natl. Acad. Sci. U.S.A.*, 2007, **104**, 14682-14687.
- 40 T. Lee, J. Park, J. Kim, S. Joo and M. Lim, *Bull. Korean Chem. Soc.*, 2009, **30**, 177-182.
- 41 V. Srajer, L. Reinisch and P. M. Champion, *J. Am. Chem. Soc.*, 1988, **110**, 6656-6670.
- 42 J. Park, T. Lee and M. Lim, *J. Phys. Chem. B*, 2010, **114**, 10897-10904.
- 43 X. Ye, A. Yu and P. M. Champion, *J. Am. Chem. Soc.*, 2006, **128**, 1444-1445.
- 44 J. Aron, D. A. Baldwin, H. M. Marques, J. M. Pratt and P. A. Adams, *J. Inorg. Biochem.*, 1986, **27**, 227-243.
- 45 S. Kim, G. Jin and M. Lim, *J. Phys. Chem. B*, 2004, **108**, 20366-20375.
- 46 M. Lim, M. F. Wolford, P. Hamm and R. M. Hochstrasser, *Chem. Phys. Lett.*, 1998, **290**, 355-362.
- 47 P. Hamm, M. Lim and R. M. Hochstrasser, *J. Phys. Chem. B*, 1998, **102**, 6123-6138.
- 48 P. Hamm, R. A. Kaindl and J. Stenger, *Opt. Lett.*, 2000, **25**, 1798-1800.
- 49 D. W. Urry and J. W. Pettegrew, *J. Am. Chem. Soc.*, 1967, **89**, 5276-5283.
- 50 W. I. White, *The Porphyrins*, Academic Press, New York, 1978.
- 51 W. Cao, X. Ye, G. Y. Georgiev, S. Berezina, T. Sjudin, A. A. Demidov, W. Wang, J. T. Sage and P. M. Champion, *Biochemistry*, 2004, **43**, 7017-7027.
- 52 D. R. Lide, *CRC Handbook of Chemistry and Physics*, CRC Press, Inc., Boca Raton, FL, 1995.
- 53 K. M. Hong and J. Noolandi, *J. Chem. Phys.*, 1978, **68**, 5163-5171.
- 54 F. C. Collins and G. E. Kimball, *J. Colloid Sci.*, 1949, **4**, 425-437.
- 55 D. Shoup, G. Lipari and A. Szabo, *Biophys. J.*, 1981, **36**, 697-714.
- 56 H. Kim, S. Shin and K. J. Shin, *J. Chem. Phys.*, 1998, **108**, 5861-5869.
- 57 H. Kim, *Chem. Phys. Lett.*, 2010, **484**, 358-362.
- 58 S. Kim and M. Lim, *J. Phys. Chem. B*, 2012, **116**, 5819-5830.
- 59 C. G. Malmberg, *J. Res. Natl. Bur. Stand. (U. S.)*, 1958, **60**, 609-612; Research Paper 2874.
- 60 A. Glycerine Producers, *Physical properties of glycerine and its solutions*, Glycerine Producers' Association, New York, 1963.
- 61 K. S. Cole and R. H. Cole, *J. Chem. Phys.*, 1941, **9**, 341-351.
- 62 G. E. McDuffie and T. A. Litovitz, *J. Chem. Phys.*, 1962, **37**, 1699-1705.
- 63 L. Onsager, *J. Chem. Phys.*, 1934, **2**, 599-615.
- 64 O. Chen, S. Groh, A. Liechty and D. P. Ridge, *J. Am. Chem. Soc.*, 1999, **121**, 11910-11911.

- 65 M. Meuwly, O. M. Becker, R. Stote and M. Karplus, *Biophys. Chem.*, 2002, **98**, 183-207.
- 66 G. E. McDuffie, R. G. Quinn and T. A. Litovitz, *J. Chem. Phys.*, 1962, **37**, 239-242.
- 67 S. Kim and M. Lim, *J. Am. Chem. Soc.*, 2005, **127**, 8908-8909.
- 68 S. Kim, J. Park, T. Lee and M. Lim, *J. Phys. Chem. B*, 2012, **116**, 6346-6355.
- 69 D. Ionascu, F. Gruia, X. Ye, A. Yu, F. Rosca, C. Beck, A. Demidov, J. S. Olson and P. M. Champion, *J. Am. Chem. Soc.*, 2005, **127**, 16921-16934.
- 70 P. Atkins and J. de Paula, *Atkins' Physical Chemistry, 10th Edition*, Oxford University Press, 2014.
- 71 M. J. Travers, D. C. Cowles and G. B. Ellison, *Chemical Physics Letters*, 1989, **164**, 449-455.
- 72 M. D. Bartberger, W. Liu, E. Ford, K. M. Miranda, C. Switzer, J. M. Fukuto, P. J. Farmer, D. A. Wink and K. N. Houk, *Proc. Natl. Acad. Sci. U.S.A.*, 2002, **99**, 10958-10963.
- 73 T. Prieto, R. O. Marcon, F. M. Prado, A. C. F. Caires, P. D. Mascio, S. Brochsztain, O. R. Nascimento and I. L. Nantes, *Phys. Chem. Chem. Phys.*, 2006, **8**, 1963-1973.
- 74 R. Margalit and A. Schejter, *Eur. J. Biochem.*, 1973, **32**, 492-499.
- 75 J. Kim, J. Park, T. Lee, Y. Pak and M. Lim, *J. Phys. Chem. B*, 2013, **117**, 4934-4944.
- 76 F. Schotte, J. Soman, J. S. Olson, M. Wulff and P. A. Anfinrud, *J. Structural Biol.*, 2004, **147**, 235-246.
- 77 M. Lim, T. A. Jackson and P. A. Anfinrud, *J. Chem. Phys.*, 1995, **102**, 4355-4366.
- 78 S. Kim, J. Heo and M. Lim, *Bull. Korean Chem. Soc.*, 2005, **26**, 151-156.
- 79 K. M. A. Refaey and J. L. Franklin, *Int. J. Mass Spectrom. Ion Phys.*, 1976, **20**, 19-32.
- 80 M. Cossi, V. Barone, R. Cammi and J. Tomasi, *Chem. Phys. Lett.*, 1996, **255**, 327-335.
- 81 R. Krishnan, J. S. Binkley, R. Seeger and J. A. Pople, *J. Chem. Phys.*, 1980, **72**, 650-654.
- 82 A. D. McLean and G. S. Chandler, *J. Chem. Phys.*, 1980, **72**, 5639-5648.
- 83 J. C. Rienstra-Kiracofe, G. S. Tschumper, H. F. Schaefer, S. Nandi and G. B. Ellison, *Chem. Rev.*, 2002, **102**, 231-282.
- 84 T. G. Grogan, N. Bag, T. G. Traylor and D. Magde, *J. Phys. Chem.*, 1994, **98**, 13791-13796.
- 85 K. Shikama, *Prog. Biophys. Mol. Biol.*, 2006, **91**, 83-162.
- 86 S. G. Kruglik, B.-K. Yoo, S. Franzen, M. H. Vos, J.-L. Martin and M. Negre, *Proc. Natl. Acad. Sci. U.S.A.*, 2010, **107**, 13678-13683.
- 87 S. Franzen, *Proc. Natl. Acad. Sci. U.S.A.*, 2002, **99**, 16754-16759.

TOC (2× scale)

Rebinding of NO to microperoxidase (Mp) via the harpoon mechanism.

